NASA Technical Paper 3020

December 1990

Large-Scale Aeroacoustic Research Feasibility and Conceptual Design of Test-Section Inserts for the Ames 80- by 120-Foot Wind Tunnel

Paul T. Soderman
and Larry E. Olson

NASA

NASA Technical Paper 3020

1990

Large-Scale Aeroacoustic Research Feasibility and Conceptual Design of Test-Section Inserts for the Ames 80- by 120-Foot Wind Tunnel

Paul T. Soderman
and Larry E. Olson
Ames Research Center
Moffett Field, California

National Aeronautics and Space Administration
Office of Management
Scientific and Technical Information Division

TABLE OF CONTENTS

SYMBOLS

b	half-thickness of acoustic splitter vane, ft
D	diameter of circular open-jet test section, ft
f	frequency, Hz
h	one-half the gap between acoustic splitter vanes, ft
L	square root of test-section cross-sectional area, ft
ℓ	channel length of acoustic vanes from aft end of nose to start of boattail, or test section length, ft
$m_{b\ell}$	mass per unit area of porous layer, kg/m^2
Δp	total pressure loss in a section of the wind tunnel, lb/ft^2
p_a	acoustic pressure absorbed by a porous layer, N/m^2
p_t	acoustic pressure transmitted through a porous layer, N/m^2
q_o	dynamic pressure in the test section, lb/ft^2
q_i	dynamic pressure at station i, lb/ft^2
R_f	specific flow resistance, mks rayls
R_{TL}	transmission loss of limp layer, dB
U	wind speed, ft/s
U_c	convection speed of vortices in open-jet shear layer, ft/s
U_o	wind speed on centerline of test section, ft/s or knots
η	pressure loss coefficient (see appendix A)
θ	angle relative to surface normal, deg
ρ_c	characteristic impedance of air, 407 mks rayls
ω	frequency, rad/s

SUMMARY

An engineering feasibility study was made of aeroacoustic inserts designed for large-scale acoustic research on aircraft models in the 80- by 120- Foot Wind Tunnel at NASA Ames Research Center. The advantages and disadvantages of likely designs were analyzed. Results indicate that the required maximum airspeed leads to the design of a particular insert. Using goals of 200, 150, and 100 knots airspeed, the analysis indicated a 30- × 60-ft open-jet test section, a 40- × 80-ft open-jet test section, and a 70- × 110-ft closed test section with enhanced wall lining, respectively. The open-jet inserts would be composed of a nozzle, collector, diffuser, and acoustic wedges incorporated in the existing 80×120 test section. The closed test section would be composed of approximately 5-ft acoustic wedges covered by a porous plate attached to the test-section walls of the existing 80×120. All designs would require a double row of acoustic vanes between the test section and fan drive to attenuate fan noise and, in the case of the open-jet designs, to control flow separation at the diffuser downstream end. The inserts would allow virtually anechoic acoustic studies of large helicopter models, jets, and V/STOL aircraft models in simulated flight. Model scale studies would be necessary to optimize the aerodynamic and acoustic performance of any of the designs. In all designs studied, the existing structure would have to be reinforced. Successful development of acoustically transparent walls, though not strictly necessary to the project, would lead to a porous-wall test section that could be substituted for any of the open-jet designs, and thereby eliminate many aerodynamic and acoustic problems characteristic of open-jet shear layers. The large size of the facility would make installation and removal of the insert components difficult. Consequently, scheduling of the existing 80×120 aerodynamic test section and scheduling of the open-jet test section would likely be made on an annual or longer basis. The enhanced wall-lining insert would likely be permanent. Although the modifications are technically feasible, the economic practicality of the project has not been evaluated.

INTRODUCTION

The trend in research on aircraft noise is toward simulation of flight effects in large wind tunnels that have been modified or constructed to have proper acoustic quality (ref. 1). The key is size and quality. Large size is important because certain aspects of powered-lift aircraft aerodynamics are difficult to simulate properly at small scale—for example, hot gas effects, boundary-layer effects, and engine-inlet mass flows. Similarly, proper helicopter-rotor Reynolds number, advance ratio, and Mach number are difficult to achieve simultaneously at small scale. For acoustics, accuracy requires that the acoustic field be probed sufficiently far from the model that the data can be extrapolated to large distances. This is very difficult if the data are acquired in the acoustic near-field, or if the wind tunnel structure or floor interferes with microphone placement. These are common problems in small wind tunnels. As for quality, it is very desirable to have minimal acoustic reflections, low background noise, minimal acoustic distortions, freedom to position microphones in almost any direction, and low turbulent flow.

An excellent facility, recently designed and built for aeroacoustic testing, is the Duits-Nederlandse Windtunnel (DNW) in Holland. This facility is the benchmark for modern aeroacoustic wind tunnels and has three interchangeable test sections, one of which is an 8- × 6-m open test section surrounded by a semi-anechoic test hall. The open jet can be replaced by a 9.5- × 9.5-m or 6- × 6-m closed jet, neither of which are acoustically treated. With this facility, the Europeans could lead the way in development of quieter rotorcraft and powered-lift aircraft. Consequently, a question is posed: Is there a need for this type of facility in this country and, if so, can we go beyond the DNW design to create an improved facility that would be complementary to the DNW? (DNW is available to American clients—at a price.)

The purpose of this paper is to examine the feasibility of developing a large, aeroacoustic test section that could be inserted into the NASA Ames 80- by 120-Foot Wind Tunnel closed test section, an idea that was conceived by researchers in the Ames Rotary Wing Aeromechanics Branch. The concept is based on the premise that the 80×120 test section is sufficiently large that an open-jet nozzle and collector, for example, could be inserted into the existing test section to create a large free jet, large enough for large-scale powered-lift or rotary-wing testing, yet small enough for far-field acoustic measurements in a surrounding anechoic test hall. No other wind tunnel exists near the size of the 80×120. Helicopter detection studies could be made using full-size or small-scale models that would allow large distances between the model and upstream microphones. Powered V/STOL models could be tested with actual power plants and without acoustic interference from floors or nearby walls. Aircraft flyover could be simulated that may provide data equivalent to FAA certification test data. Acoustic investigations could be made of advanced jet engines such as will be required for the new supersonic transport concepts. Finally, the cost of developing a complete wind tunnel including drive system would be avoided.

The modification, however, would be complicated by the following requirements:

(1) The utility of the existing 80×120 must not be compromised; to achieve this, the insert may have to be removable.

(2) Duct silencers must be incorporated to reduce noise from the fan-drive downstream of the test section.

(3) The walls surrounding the test section will have to be lined with acoustic wedges or other sound absorbers.

(4) The flow into the fans must not be overly distorted.

Preliminary assessments are presented of the acoustical attributes, aerodynamic performance, facility pressure loads, and logistical aspects of the most promising designs. Proper implementation of these ideas will hinge on extensive small-scale simulations of the aerodynamic and acoustic characteristics of the facility. Certain research areas have been identified that might, if exploited successfully, lead to an aeroacoustic test section superior to the classical open-jet or closed-jet wind tunnel. For example, a test section with walls that are acoustically transparent, yet restrict airflow, might be better than an open or closed jet. Such a concept has been investigated with some success in a small-scale wind tunnel, as will be discussed in Part 3.

Early in the study, it became clear that airspeeds greater than the present maximum of 100 knots in the 80×120 would be desirable for aeroacoustic research of many classes of aircraft. For example, new supersonic and hypersonic aircraft will land at speeds approaching 200 knots, and the jet noise directivity is sensitive to forward speed. Similarly, high-speed helicopter noise should be studied at speeds greater than 100 knots.

Therefore, consideration was given to a new contraction leading to an open jet or closed jet inside the existing wind tunnel envelope. Since different speed goals lead to different insert designs, this report has three sections that address the conceptual design of aeroacoustic inserts for maximum airspeeds of 100-, 150-, and 200-knots. In addition, the report contains a section on the required duct silencer, and a section on miscellaneous components, airloads, logistics, etc. It was not the purpose of this study to define the optimum airspeed; that decision must be made in light of the overall research goals of NASA. Consequently, the single, best test-section insert has not been defined.

The Existing 80- by 120-Foot Wind Tunnel

The Ames 80- by 120-Foot Wind Tunnel (refs. 2 and 3) is a non-return, closed-test-section wind tunnel that shares the same fan-drive system as the 40- by 80-Foot Wind Tunnel as shown in figures 1(a) and 1(b). When operating in the 80×120 mode, large vanes close off the 40×80 circuit so that the airflow enters the 80×120 inlet, passes through the test section via a 5-to-1 rectangular (conical) contraction, through two vane sets, one of which turns the airflow 45°, through the fan drive, and out the exhaust in the south end of the facility. The various vane sets used to close off the 40×80 circuit and turn the airflow into the drive fans are illustrated in figure 1(c). The inlet contains acoustically treated flow-straightening vanes and a turbulence dampening screen as shown in figure 1(d). The rectangular test section is 80-ft high, 120-ft wide (not counting the 10-in. sound-absorbent wall lining and 6-in. floor/ceiling lining), and roughly 300 ft long.

The models are mounted to balance struts centered on a 60-ft diameter turntable. The turntable and a telescoping tail strut are used to control model angle of attack and angle of yaw. Three components of force and three moment components can be measured on large models. Smaller models can be equipped with load cells for measurement of aerodynamic force and moments. The center of the turntable is 156 ft downstream of the inlet contraction termination.

The test section wall linings, composed of fiberglass bats wrapped in cloth and covered with a 40%-open-area perforated steel plate, are designed to absorb and thereby attenuate model noise propagating through the walls or out the inlet and exhaust, and to reduce reflections so that acoustic studies can be made of powered models. The side-wall lining is 10 in. thick, and the floor and ceiling linings are 6 in. thick. Figure 2 illustrates the acoustic lining geometry. The sound absorption has not been measured *in situ*, but laboratory and wind tunnel tests (refs. 4 and 5) indicate that the lining will absorb 70% or more of the incident acoustic energy for frequencies above 80 Hz, in the case of the side walls, and 125 Hz, in the case of the floor or ceiling. This is not adequate for some large-scale rotorcraft which have important low frequency noise sources; better absorbers will be needed for tests of low-frequency models.

The fan drive is the primary source of background noise in the test section. Six 40-ft diameter fans are located in the wind tunnel drive section in two horizontal rows of three fans each (fig. 3). The fans were designed with low tip speed (377 ft/sec at 180 rpm) for minimum noise. In addition, the inflow has been improved, and the number of rotor and stator blades was chosen to minimize modal propagation. Nonetheless, the fans are partially visible from the test section and therefore generate considerable background noise, as will be presented in a later section. Table 1 lists the principal geometric and operating characteristics of a single fan. The fans can be operated from 0 to 180 rpm and with blade-pitch angles from −18° to 52° relative to the fan disc. The maximum mass flow results in a speed of approximately 100 knots in the 80×120 test section.

Existing Large Open-Jet Wind Tunnels

In the first half of this century, a number of large open-jet wind tunnels were constructed, such as the NASA Langley 30- by 60-Foot Wind Tunnel, the ONERA S1 at Chalais-Meudon, and the RAE 24-Foot Wind Tunnel. Those facilities have served well for low-speed aerodynamic research. Though they are still used for certain specialized testing, they have been largely superseded for general aerodynamic research by closed and slotted wind tunnels which operate with more effi-

ciency and with smoother airflow than open jets. In more recent times, however, a number of open-jet wind tunnels, both large and small, have been developed for the dual purpose of aerodynamic and acoustic research on aircraft. It is important to note that the aerodynamic performance of these facilities is generally inferior to closed- or slotted-test-section wind tunnels because of the high flow losses and induced turbulence inherent in an open jet. Nevertheless, the open test section can be integrated with a large anechoic test hall surrounding the jet that can provide an acoustic advantage over the classical closed-jet wind tunnel for the reasons mentioned above. Thus, the open-jet has regained an important purpose for aeronautics research.

There may be a number of ways to classify open-jet wind tunnels, but since they are all subsonic the most obvious way is by size. The NASA Aeronautical Facilities Catalogue (ref. 6) classifies subsonic wind tunnels into 10 groups. Group A includes wind tunnels with a test-section dimension (diameter or the smaller of height and width) greater than 30 ft. Group B includes wind tunnels with a test-section dimension between 12 and 30 ft. Those facilities can accommodate model scale from 1/4 to full scale. It is these two categories that concern us here, because there is a lack of such facilities in the U.S. suitable for large-scale acoustic testing.

Table 2 lists the large open-jet wind tunnels (Groups A and B) in the free world, along with their test-section sizes and speeds. They are all low-speed facilities. The DNW Wind Tunnel has a top speed of 150 knots, the highest speed of the group. Mort et al. (ref. 7) suggested that a large-scale wind tunnel speed of 300 knots would satisfy most airspeed requirements for large-scale aerodynamic testing. Although some types of acoustic testing can be satisfactorily done at low speeds, airspeeds below 100 knots are inadequate for proper simulation of certain high-speed acoustic-source mechanisms of modern V/STOL and helicopter aircraft. Thus, a goal of 100-200 knots maximum airspeed was chosen for this feasibility study.

Of the wind tunnels listed in table 2, only the DNW facility was designed and built for both aerodynamic and acoustic testing. The other wind tunnels were originally designed for aerodynamic research and, consequently, have acoustic deficiencies such as high background noise and reflections. Focusing on three of the facilities in this country listed in table 2, the NASA Langley 30- by 60-Foot Wind Tunnel has two drive fans very close to the test section (two fan diameters downstream) which generate high levels of background noise in the test section (ref. 8); the NASA Langley 14- by 22-Foot (refs. 8 and 10) and the Boeing Vertol 20- by 20-Foot (ref. 8) also have high background noise levels. Considerable effort (refs. 9 and 10) has gone into identifying the sources of background noise in the 14×22, as well as finding methods to smooth the flow in the open jet. With modifications, that facility could become an important research tool for aeroacoustic testing of V/STOL and helicopter models. The primary limitations would be its relatively small size, low flow speed, and floor reflections.

Conceptual Design Procedure for the Acoustic Insert

In order to evaluate the feasibility of an acoustic test section in the 80×120, it is necessary to define, in general terms, the most likely geometry. This is an iterative process involving acoustic, aerodynamic, and geometric requirements. For this study, the following design steps were found to be most effective. Steps 3 to 7 apply only to the open-jet designs.

(1) Set test-section maximum air speed at 100, 150, or 200 knots.

(2) Define depth of wedges for existing duct walls so that 99% of acoustic energy above 60-Hz will be absorbed. That depth is about 5 ft. The 60 Hz design frequency is arbitrary and can be lowered by using deeper wedges. Longer wedges, say 5 to 10 ft long, would have a weak influence on the test-section design. Choose a perforated cover plate for those designs which have an acoustic lining exposed to the airflow.

(3) Define the maximum nozzle area that will achieve the desired airspeed while maintaining a minimum distance of 15 to 20 ft from the shear-layer outer edge to the acoustic wedges.

(4) Locate the nozzle streamwise so that the jet-core-flow width at the model will be 80 to 90% of the nozzle width. The model will be at the center of the existing turntable.

(5) Locate the jet-collector lip such that unobstructed acoustic measurements can be made from 30° to 145° from the model center (horizontal or vertical plane) relative to the upstream direction.

(6) Define the collector shape and throat location required to capture the jet while maintaining stable flow with low pressure loss.

(7) Define the maximum diffuser angle that will result in unseparated flow in the diffuser. Because of the relatively short length of the existing 80×120 duct, the proposed diffuser must be truncated at the downstream end and will have flow separation at that point. This is a relatively high-risk item since separated flow could result in unacceptable speed losses and could induce large, unsteady loads on the drive fans.

Model scale testing will be required to resolve this problem.

(8) Design an acoustic vane set for adequate attenuation of fan-drive noise with acceptable flow loss.

(9) Estimate system flow loss and test-section airspeed. Alter the design geometry and return to step 1 as necessary.

It should be noted that the control of flow oscillations implied in step 6 can only be verified experimentally. Since existing large open jets develop flow oscillations at or below 150 knots, the design goal of 200 knots may not

be achievable. The analysis required to perform the above design iteration is described in the following sections.

PART 1 – 30- BY 60-FOOT OPEN-JET WIND TUNNEL FOR 200 KNOTS AIRSPEED

The open-jet test section is the obvious choice for achieving 200 knots, since a new contraction and throat would leave considerable space between the test section and surrounding 80×120 walls. That space would lend itself well to use as an anechoic room for placement of microphones outside the flow, relatively far from the model.

Furthermore, acoustic reflections striking microphones inside the flow would be much easier to attenuate in an open jet than in a closed jet since the reflecting walls in the anechoic room could be well treated. A key part of the open-jet design is the definition of the jet shear layer.

Open-Jet Shear Layer

Acoustic Interference– The shear layer between an open-jet flow and quiescent air outside the test section is both helpful and unhelpful. It is helpful because it allows the aircraft-model noise to propagate out of the flow with little reflection, at least for the low speeds and propagation directions used in typical facilities. Thus, an acoustic-free field can be established and sampled in or out of the flow. The disadvantage of the shear layer is twofold–aerodynamic and acoustic. First, turbulence and vortices in the shear layer perturb the core flow in the jet and can, under certain conditions, interact with the collector and nozzle in such a way as to cause the entire jet to oscillate, sometimes violently. Jet oscillations can also couple with room-acoustic modes. Furthermore, the entrainment of air causes significant recirculation flows in the acoustic hall. Second, the shear layer distorts, scatters, and refracts the transmitted sound, depending on propagation angle, flow Mach number, and acoustic frequency.

Methods have been developed to successfully correct for refraction; for example, the method developed by Amiet (ref. 11). Amiet models the shear layer as a thin interface and predicts the acoustic-ray refraction as illustrated figure 4. The solid line represents the refracted acoustic ray; the dashed line represents the propagation path of the same ray propagating in a uniform velocity field without a shear layer. The true directivity of a point source can be deduced from measurements of apparent directivity since the refracted angle of a sound ray can be predicted from the angle at which the ray strikes the shear layer.

However, the situation is much more complex with a large noise source and a nearby observer because the observer cannot be sure where the sound originated; the ray/shear layer intercept angle is ambiguous. Sound from a distributed source observed at one point in a uniform velocity field will be spread by the introduction of a shear layer as illustrated in figure 4. Although the acoustic spread is not nearly as severe in the downstream direction as upstream, the complete directivity pattern of a distributed source may be hopelessly distorted by the shear layer. To eliminate this problem it would be necessary to move the microphones into the far-field where the distributed source looks like a point source. Or, if one had high confidence in the shear-layer refraction model, it might be possible to place the microphones at points where the acoustic rays coalesce outside the jet as illustrated in figure 4. This is an interesting concept because, in theory, every acoustic ray that arrived at the receiver location without a shear layer would focus at a single displaced point if a shear layer were introduced. It does not matter where the ray originated on the source. Data acquired at that focus point could be used to reconstruct the original acoustic radiation without shear layer.

Methods (refs. 12 and 13) have also been proposed to deal with spectral broadening, amplitude fluctuations, and phase fluctuation. However, impulse signatures can be severely distorted in time and phase by the shear layer. Consequently, many researchers studying rotor noise, for example, prefer to place their microphones inside the open jet despite the limitations imposed by the near acoustic field. The conclusion, therefore, is that research must continue on the effects of the shear layer on propagating sound, and efforts should be made to minimize and control the shear layer to avoid disturbances to the acoustic field and flow field. Furthermore, efforts should be made to find an alternative to the open-jet shear layer, such as the acoustically transparent wall discussed in Part 3.

Shear-Layer Spread– The design and location of the collector, the size of the free-jet area and model size, the test-section flow quality—all depend on the expansion of the open-jet shear layer as the jet moves downstream. Calibrations of many round jet flow fields have shown that the mixing layer closes on itself at about five jet diameters (e.g., ref. 14). In other words, the potential core is a conical region with the apex about five jet diameters downstream from the nozzle. That implies that the shear layer spreads over approximately 11° total angle with the origin at the nozzle lip. This is somewhat less than the angle given by the analytical model of Abramovich (ref. 15), which indicates that the circular jet with uniform velocity distribution spreads at 15.4° or, relative to the nozzle-lip line, 6.4° into the jet and 9° away from the jet. Rebuffet and Guedel (ref. 14) measured the cross-stream velocity distribution downstream of the CEPRA 19 Anechoic Open Jet Wind Tunnel and showed that the shear layer of that round jet spread over a total angle of 11.7°, as shown in figure 5. The potential core is taken to be that region where the mean velocities were at least 99% of the centerline velocity. (Turbulence distributions are reported in ref. 16.)

The data of Van Ditshuizen et al. (ref. 17) indicate that the rectangular-jet shear layer spreads at a different rate than a round-jet shear layer. Their calibration of the DNW 8- × 6-m open jet shows that the shear layer spreads over a total angle of 8.2°. This is 3° to 4° less than that of a round jet. Again, the shear layer was defined as the mixing layer outboard of the potential core where the mean velocities are at least 99% of the centerline velocity. In fact, the shear layer influences the flow outside the 8.2° wedge-shaped region because of the unsteady velocities induced by vortices moving in the shear layer. Boxwell et al. (ref. 16) illustrate this in comparisons of the flow properties of CEPRA 19 and DNW along with the aeroacoustic implications. The DNW calibration data (refs. 17 and 18) in figure 6 show longitudinal and lateral turbulence distributions in a cross section 7 m downstream of the 8- × 6-m nozzle exit. The locations of the horizontal and vertical survey points are shown as a row of dots on each graph. The region of low turbulence is only 40-50% of the potential core width, as defined above, and outside that region the turbulence increases rapidly. In other words, the potential-core mean velocities were within 1% of the centerline velocity, but the turbulence in much of that region was increased by the shear layer. The influence of the shear layer, therefore, is important over a total angle of approximately 32°. This is a fundamental problem with open jets and may or may not be important for potential users of such a facility, depending on the specific model size and test requirements. For this design study, an 8° shear-layer total angle corresponding to the limits of good mean flow will be used.

Test Section and Nozzle Size for 200 knots Airspeed

The purpose of this section is to define the largest open-jet test-section insert practicable in the existing 80×120 closed test section that meets the 200-knots airspeed requirement and acoustic requirements. That insert would allow large-scale aeroacoustic simulations with the resulting advantages of large size (ref. 1). A lower limit on test-section cross-sectional area depends on the acoustic requirement to measure noise in the acoustic far-field of the source. In general, the microphone to model distance should be greater than each of the following dimensions: (a) one acoustic wavelength, and (b) two source lengths, the source length being the largest distance between any two noise sources on the model (ref. 17). Thus, if a full-size helicopter in the 80- by 120-Foot Wind Tunnel had a rotor diameter of 50 ft, for example, microphones could not be placed in the acoustic far-field to the side or below the helicopter because of the walls (for an acoustic source related to the rotor diameter), although microphones could be placed upstream or downstream of the model. The blade-passage frequency of full-size rotors corresponds to a wavelength on the order of 20 to 50 ft, which also could be a problem for microphone placement. So, a test section large enough to accommodate a 50 ft rotor, for example, would be unnecessarily large since the acoustic far field of the rotor would be severely restricted by the 80×120 walls.

Another limitation on test-section area is the need to have an adequate open space between the jet and the walls of the test chamber for microphone placement outside the flow, even though microphones could and would be used in the flow. The microphones outside the flow cannot be placed too close to the sound-absorbent wedges on the walls because of local reflections. (The wedges will be about 5 ft long, as described later.) The microphones cannot be placed close to the nozzle or collector, even though those two components would be acoustically treated. Nor can microphones be placed close to the shear layer because of its inherent noise and induced flow. A reasonable open space for the microphones would be around 20 ft between the shear layer and the wedge tips. At DNW, the free space to the side and below the test section is approximately 40 ft and 20 ft, respectively.

Based on these acoustic requirements of model size, acoustic wavelength, and microphone location, the appropriate maximum open-jet nozzle size for a 200-knots airspeed would be around 30-ft high by 60-ft wide as shown in figure 7(a). Rotorcraft-model scale would be on the order of one half. This would give a shear layer to wedge tip clearance of 17-25 ft to the side and 12 to 20 ft above and below the test section. The smaller clearance above and below the test section can be justified by the need to maximize the region of smooth flow for lifting rotors and wings. At the turntable center, the core flow is only 22-ft deep and 53-ft wide as shown in figure 7(a). For comparison, clearance around a 40×80 jet are shown in figure 7(b). At the turntable center of that test section, the core flow is 29-ft deep and 69-ft wide, but the clearance between the shear layer and wedges is only 10 ft.

The open-jet length is dictated by (a) the need to have smooth flow over the model, and (b) the need to have an adequate acoustic arena outside the jet for acoustic directivity measurements. Item (a) determines the distance from the model center to the open-jet nozzle since the shear layers cannot be allowed to spread into the model.

Because most models would be mounted at the turntable center, the nozzle should be around one nozzle-width upstream of the turntable center. With a shear layer spread of 8° total angle, the free-jet width at the model would be 0.86 of the nozzle width. Of course, the model span would have to be significantly less than the free-jet width to minimize "wall" effects.

Item (b) locates the collector lip since the acoustic radiation field is bounded by the nozzle on the upstream side of the model and the collector lip on the downstream side. A reasonable goal would be to maintain a free field from 30° to 145° measured from the turntable center, 0° being the upstream direction. That would barely allow capture of peak sound levels from jets, which are maximum near 140°. Many categories of propeller or rotor noise would radiate outside the flow. Some types of noise such as high-speed helicopter noise, however, radiate forward and would have to be captured inside the test

section. Suitable nose cones can be used to protect the microphone and minimize wind noise, although improvements in noise-cone design are desirable. Usually, the microphones would be downstream of the nozzle, but in some cases microphones would be placed upstream of the nozzle near the 80×120 inlet guide vanes. With these constraints, the open test-section length will be on the order of 110-120 ft. The exact length will depend on the collector geometry described in the following section.

Collector and Diffuser

Most open-jet wind tunnels have collectors designed to capture the free jet and feed the airflow into a diffuser downstream. The diffuser then allows the air to decelerate and recover its static pressure as it moves toward a drive fan. Aerodynamically, a free-jet collector must capture the jet and shear layers as smoothly as possible to avoid pressure fluctuations in the test section. Abramovich (ref. 15) showed analytically that the collector should just capture the jet-core mass equal to that emitted from the nozzle in order to avoid a longitudinal *static* pressure gradient in the test section (not to be confused with unsteady pressure). Entrained flow in the shear layer would be cut off. In practice, however, this would require a collector immersed in the shear layer. Such a collector would experience strong *unsteady* pressure fluctuations which can radiate upstream acoustically, and trigger vortex shedding from the nozzle lip that can create flow oscillations at resonance conditions (ref. 19). Thus, the collector leading edge should not intrude too far into the shear layer. (Likewise, a collector that is too large will result in unnecessarily high flow losses as discussed in the following section on Open-Jet Flow Losses.)

Based on published reports and discussions with wind tunnel designers and operators, it is likely that all open-jet wind tunnels built to date develop flow oscillations at some flow speed, and, if flow speed is further increased, those oscillations can grow to violent levels. This may be a fundamental limitation of the open-jet wind tunnel. The oscillations are created by a feedback loop involving unsteady pressures on the collector or diffuser, which radiate acoustic waves upstream, which in turn trigger vortex shedding from the nozzle, which creates unsteady pressures on the collector or diffuser, and so on. The mechanism has been reported by Rebuffet and Guedel (ref. 14) to be an edge-tone type resonance with the following frequency dependence on vortex convection speed in the shear layer, U_c, and length of the open jet, ℓ:

$$f = (n + 1/4)\, U_c/\ell \qquad \text{where } n = 1,2,3 \ldots \qquad (1)$$

Using an open-jet test section length of 120 ft and a convection speed (ref. 14) of 0.54 U_o, where U_o = 338 ft/s (200 knots), the frequency given by equation (1) is only 1.9 Hz for n = 1. Thus, the flow oscillations in the proposed test section would have a very low frequency that would affect flow quality and might perturb models such as helicopters. If the flow oscillations couple with an acoustic or mechanical room mode, structural failure of the facility can follow. Typical speeds at which strong flow oscillations begin are in the neighborhood of 150 knots, although each facility is different.

To delay the onset of flow oscillations, two methods are available. The first is to install vortex generators on the nozzle lip, as is done at several facilities. Martin et al. (ref. 19) developed triangular vanes which dramatically reduced dynamic pressure and turbulence fluctuations in the Langley 14- by 22-Foot Wind Tunnel. To control vane noise, they used foam material, flow trips, cavity plugs, and special streamlining.

However, the vanes caused the required fan power to increase 30% and reduced the size of the uniform flow in the test section.

The second method to control open-jet oscillations is to optimize the collector shape. NASA Langley has developed a three-sided collector for the 14- by 22-Foot Wind Tunnel illustrated in figure 8. That collector has flat surfaces separated from the diffuser by a 6-ft gap (adjustable to 1.5 ft). The gap was optimized for minimum turbulence in the test section (ref. 20). The side walls are set at 14.5° to the free stream, and the top is set 6° to the free stream. In retrospect, the top angle could have been greater in order to avoid unnecessary air spillage (private communication with Zachary Applin, NASA Langley Research Center). Therefore, 14.5° will be used for collector sides, top, and bottom in the design proposed here. The Langley collector stabilizes the flow in the jet sufficiently so that the nozzle vanes are not needed. Figure 8 shows that a line connecting the nozzle lip and collector lip (sidewall) is 7° from streamwise. A line from the nozzle lip to the collector throat is only 1° from streamwise in the plan view and around 0° in the elevation. These various dimensions and angles are important to the initial design of the collector for the proposed 80×120 insert.

Figure 9 shows the DNW collector geometry which is similar, but not identical, to the collector in the Langley 14- by 22-Foot Wind Tunnel. It is proposed that the DNW or Langley design would be a good starting point for the experimental development of a collector for an open jet in the 80×120, although it is possible that the optimum collector for each facility is unique.

Open-Jet Flow Losses– It would be advantageous for acoustics if the open-jet test section were long. However, this affects the flow losses. The flow losses of an open-jet wind tunnel are caused by the loss of kinetic energy in the core flow as it mixes in the turbulent shear layer between the core flow and quiescent air outside the jet. In this process there is also energy lost as the jet entrains air or gives up air to the volume outside the jet, a mechanism which can drive large circulating flows in the room outside the jet. If the test chamber surrounding the jet is ventilated, the entrained flow adds mass flow to the jet and reduces the local test-section loss, but the drive fan must produce more energy to propel the entrained flow along the duct.

Consequently, the aerodynamic losses of an open-jet test section are much higher than a closed-jet test section as shown by Idelchik (ref. 21) in figure 10. (Loss coefficient is defined in appendix A.) Idelchik also predicted how the open-jet losses go up as the length of the open section increases (fig. 10). However, it is not clear how the losses depend on the cross-stream location of the collector; that is, where the collector throat (i.e., the diffuser inlet) is located relative to the shear-layer width. For flow stability, it might be argued that the collector throat should be as far outboard as possible, since impingement of a strong shear layer on the collector can cause acoustic-pressure feedback to the nozzle and generate oscillations. However, the increased volume of circulating flow will drive the flow losses up, and the hall outside the jet would have to be vented to allow entrainment. Since the DNW and Langley 14- by 22-Foot Wind Tunnels have collector throats with a cross section similar to the nozzle cross section, that arrangement will be recommended here.

According to J.D. Vagt of Porsche (unpublished presentation at Subsonic Aerodynamic Testing Assoc. 23rd Annual Meeting, Palo Alto, Calif., June 10, 1987), an open-jet test section which is too short can result in incorrect drag measurements from vehicles. This is caused by deformation of streamlines and a longitudinal pressure gradient as the flow passes the body and curves into the collector. Vagt recommends that the ratio of open-jet length to hydraulic diameter be greater than 2.96. (For a wind tunnel, hydraulic diameter equals four times the duct cross-sectional area divided by the perimeter.) For a 30×60 open jet, the hydraulic diameter is 40 ft, and the recommended minimum open-jet length according to Vagt's criterion is 118 ft.

Using the open-jet loss factors of Idelchik (ref. 21) summarized in appendix A, the wind-tunnel circuit losses were estimated. Tables 3-5 list the component losses for: (a) the baseline (unmodified) 80- by 120-Foot Wind Tunnel (table 3), (b) a 30×60 insert (nozzle, collector, and diffuser) with a 120-ft long test section (table 4), and (c) a 30×60 insert with a 150-ft long test section (table 5). The open-jet test-section loss coefficient is computed in appendix B from DNW unpublished data on power required versus test section speed (Compilation of Calibration Data of the German-Dutch Wind Tunnel, MP-82.01, March 13, 1982, by the staff of DNW) and is similar to the coefficient given in reference 21. The wind-tunnel speed is limited by either maximum fan power available (135,000 hp for six fans), or by maximum pressure rise through the drive fan (55 lb/ft^2). A higher fan pressure could cause the fan to stall. The estimated test section loss increased from 7% of the total circuit loss for the closed 80×120 test section to 71% for the 30×60 insert (see tables 3 and 4).

These flow losses can be illustrated in terms of test-section speed as shown in figures 11(a) and 11(b). Figure 11(a) is a comparison of the 120-ft long 30×60 open jet with the baseline 80×120 closed jet. Despite the higher losses of the open jet, the reduced test-section area creates a maximum jet speed in the 30×60 more than twice that of the 80×120. The limit of 219 knots in the 30×60 was reached when the fan-pressure rise limit of 55 lb/ft^2 was reached. (This speed will go down when the acoustic-vane set loss is included.) The 80×120 top speed of 108 knots is limited by the available fan power of 135,000 hp. Figure 11(b) shows that the 150-ft long open jet would decrease the maximum flow speed in the test section to 195 knots. Again, the fan-pressure rise limit was reached. Thus, there would be a 11% speed penalty for the longer test section.

The addition of the acoustic vane set between the open jet and fan drive, to be described in Part 4, increases the losses and reduces the test-section speed as tabulated in table 6. Figure 12 shows that the 30×60 nozzle with 120-ft long test section would have an approximate top speed of 197 knots when the loss of the acoustic vane set is included. Thus, the 30×60 is the largest open-jet test section that will (approximately) achieve the goal of 200 knots top speed. Details on the acoustic-vane set and calculated losses are described in the sections entitled Fan-Drive Silencers and Acoustic Vane Pressure Row Loss. One effect of the increased loss, relative to the existing wind tunnel losses, is to push the fan toward stall. Model scale testing would be required to verify that adequate stall margin exists. If it does not, the maximum speed of the facility would have to be reduced below 200 knots, or the size and length of the test section would have to be reduced to achieve 200 knots.

Figures 13(a)-13(c) summarize the test-section and collector/diffuser geometry derived so far. The collector throat is located about 120 ft from the nozzle to give an adequate acoustic measurement arena outside the jet. That test section would allow far-field acoustic measurements from 32° to 146° to the side of the model (0° is the upstream direction) and from 19° to 154° below or above the model. Longer test sections would result in flow losses and subsequent air-speed reductions below the goal of 200 knots top speed. The width of the collector throat would be around 60 ft, and the height would be around 30 ft. A smaller collector might aggravate the shear-layer oscillation problem, and a larger collector would squeeze the surrounding test hall and increase the flow losses. The collector would entrain air into the diffuser if the surrounding room were ventilated. Circulating flows would be created in the surrounding room with or without ventilation, but the recirculation would likely be strongest without ventilation. Whether or not the room should be ventilated will depend on small-scale studies used to examine the tradeoffs between entrainment, recirculation, and flow losses. The optimum collector size and position would have to be verified experimentally. It should be noted that it will also be necessary to experimentally assess the effect of high-lift models on flow into the collector.

Diffuser– Because of the relatively short length of the existing 80×120 duct, the open-jet diffuser shown in figures 13(a)-13(c) has a truncated downstream end.

Idelchik (ref. 21) developed diffuser-loss estimates for truncated diffusers as outlined in appendix A.

Despite the aerodynamic uncleanliness of the truncated diffuser, the flow losses can be kept moderately low by using small diffuser wall angles so that the flow does not separate until it reaches the truncated end. Closed wind tunnel design guides (ref. 22) indicate that a diffuser half-angle around 4° (angle of one wall relative to duct axis) is the maximum recommended. This results in as short a diffuser as possible without compromising diffuser efficiency or creating unacceptable flow separation. The DNW diffuser wall angle (ref. 17) is 4.1°. These guides, along with the formulas of Idelchik in appendix A, lead to a 4° wall angle for the recommended diffuser design.

Even with acceptable flow losses, the truncated diffuser could create serious problems for the drive fans if the large, separated flow regions carry into the fans. The turbulence and distorted inflow could induce unsteady blade loads that might be unacceptable from a structural and acoustic standpoint. These effects are difficult to predict and, therefore, would have to be examined experimentally.

Another factor in the diffuser design is the aerodynamic influence of the acoustic vanes required to block fan noise. Two vane rows will be needed in the downstream end of the diffuser, as will be described in the section on Fan Drive Silencer. Although the primary function of these vanes is acoustic, they could also be used as flow control devices so that a greater diffuser wall angle could be tolerated (ref. 23). Furthermore, it may be possible to splay the vanes and spread the flow outboard to minimize the separated flow regions behind the truncated diffuser and prevent spoiled flow from entering the fan drive. Once again, it is clear that effective utilization of the acoustic vanes as flow-control devices will require additional analysis and scale-model testing to optimize the geometry. At this point, it is not possible to predict the flow effects of the vane rows with enough confidence to change the recommended wall angle of 4°.

Acoustic Test Hall

Wedges– Acoustic wedges will be required on certain areas of the test hall surrounding the open jet in order to achieve anechoic conditions. Other less critical areas can be covered with flat, absorbent liners. The current trend in wedge design in this country is to use polyurethane or similar foam material instead of fibrous materials because of the tendency of fibrous wedges to shed fibers over time, especially if the wedges have to be handled or contacted for any reason. The DNW facility, however, employs mineral wool wedges and liners (ref. 24). The wall wedges are only 2.62 ft deep mounted over a 0.33-ft air gap, yet are reported to have 99% sound absorption down to 80 Hz; the floor wedges are 3.28 ft deep without an air gap. All DNW wedges are protected by cloth and wire mesh.

Foam wedges are easily cut into shape and are more durable than fibrous wedges. Foam density and reticulation (rupture of cell walls) can be controlled to a certain extent so as to create a desired acoustic impedance. The primary drawback to polyurethane is that it is flammable and gives off poisonous gases when burned. It can be treated with fire-retardant chemicals; however, the life of such chemicals is uncertain. An automatic sprinkler system could be installed for fire control. Polyurethane is used in many acoustic applications safely, but this would not be advisable below powered models which can drip fuel. Those areas would require nonflammable material.

The wedge shape is critical to the sound absorption because it forces reflections from the wedges to strike the neighboring wedge rather than reflect back toward the source, as happens with flat panels. Even blunt wedge tips must be avoided to prevent high-frequency reflections back into the room (ref. 25).

The usual absorption criterion is that the wedges must absorb 99% of the incident acoustic energy above some lower frequency limit. Since such high absorption in foam wedges is usually only possible for acoustic wavelengths less than approximately four wedge depths, the necessity to eliminate wall reflections above 60 Hz in the test hall (an arbitrary goal) means that the acoustic wedges must be approximately 5 ft deep. For this depth, it may be necessary to install a slender, inner support in the wedges to prevent drooping. Below 60 Hz, absorption will decrease as frequency decreases. Alternatively, a careful development program could lead to much shorter wedges, such as the DNW 3.28-ft mineral wool wedges, which have optimum impedance and, therefore, excellent absorption.

Wedge absorption depends on the flow resistivity and density. Typical values of flow resistivity for this application would be 2,000 to 10,000 mks rayls/m. There is considerable leeway on that parameter, but the optimum value would have to be determined by parametric testing in a large standing-wave tube. The density would be chosen high enough so that the wedges would be adequately robust, yet not so high that the flow resistance would be too large. A typical value for foam wedge density is 2.2 lb/ft^3.

Both the collector and nozzle should be lined with absorbent material to minimize acoustic reflections. Flat liners can also be used on the test arena walls in non-critical areas where wedges are not necessary, but sound absorption is still desired. Foam blankets can be employed, but for optimum performance, DNW uses multiple layers of mineral wool, each layer having a desired density and impedance (ref. 24). The total DNW liner depth is 0.66 ft.

Acoustic Arena Geometry– As shown in figures 13(a)-13(c), the acoustic arena surrounding the test section is relatively small compared to the test section. However, there is approximately 17 to 25 ft between the 30×60 shear layer and wedge tips on the side walls, and approximately 12 to 20 ft between the shear layer and wedge tips above and below the test section. This is less

than the design goal of 15-20 ft, but increasing the free space above and below the model means reducing the test-section height and consequently reducing allowable model size. Fixed or traversing microphones could be placed around 50 ft from the test-section center to the sides, and around 30 ft from the test section center, above and below. The closest microphones (i.e., at the same streamwise location as the model) would be in the acoustic far-field for models with acoustic sources separated around 20 ft. At microphone locations downstream or upstream, larger models could be accepted without violating the far-field limits. Microphones outside the jet could sample far-field sideline noise from 32° to 146° from the upstream direction, measured from the turntable center, and 19° to 154° below the model, although the data at the limits of that range would be affected by acoustic refraction and reflection from the nozzle or collector.

A novel way to increase the source-to-microphone distance would be to open the two large doors on the east wall of the 80×120 and place the microphone outdoors.

The door opening is 80-ft high by 120-ft wide. If that opening did not adversely affect the open-jet flow too badly, it might be possible to place microphones at angles from 45° to 135° relative to the upstream direction, at distances up to 200 ft from the model center. This would probably be feasible only at low speeds.

For acoustic detection studies of aircraft, microphones could be placed upstream of the model and open-jet nozzle. The maximum distance from the model would be 306 ft, which is the distance to the 80×120 inlet guide vanes. Reflections from the vanes will restrict the actual microphone placement, but this could be investigated easily using impulsive noise sources in the test section. Reflections from the nozzle would also be a problem unless steps were taken to acoustically treat the nozzle surface. One way to avoid reflections would be to use directional microphone arrays that would focus on the model and reject reflections from the nozzle or inlet vanes. An end-fire array (ref. 26) will have a directional response shaped like a flashlight beam. The beam width can be tailored by optimizing the number of array elements and element spacing.

Air circulation in the measurement hall induced by the open jet can cause vibrations and wind noise on the microphones. The circulation patterns and velocities can best be determined experimentally with a scale model of the facility.

PART 2 – 40- BY 80-FOOT OPEN JET FOR 150 KNOTS AIRSPEED

The primary advantage of a 40×80 open jet is that models sized for that test section could be operated in the closed 40- by 80-Foot Wind Tunnel or vice versa. However, that test section size leaves approximately 10 ft between the shear layer and the wall wedges at the model center, which is inadequate for proper separation between the microphones, shear layer, and wedges as shown in figure 7(b). On the other hand, there is more room for inflow microphones than there would be in the 30×60 design. Unfortunately, models sized maximally for the 40×80 test section would likely be too close to the microphones to the side or under the model for acquiring far-field acoustic data from large source regions. Microphones could be placed upstream or downstream of large models and be in the acoustic far field. Based on the methodology described in the preceding section, the geometry of the 40×80 insert is shown in figures 14(a)-14(c). The estimated maximum airspeed would be 155 knots based on the flow losses tabulated in table 7.

PART 3 – TWO CLOSED JETS FOR 100 KNOTS AIRSPEED

The most simple modification to the 80- by 120-Foot Wind Tunnel would be to create an anechoic space in the existing test section. The maximum airspeed would then be close to the present 100 knots. Unlike the open-jet designs, all microphone locations would be exposed to airflow.

Enhanced Wall Lining

Sound-absorbent wall linings have been used in various wind tunnels for acoustic research, including the 40- by 80-Foot Wind Tunnel, which has a 6-in. lining permanently installed in the test section. All the aerodynamic, acoustic, and logistic problems of an open-jet insert could be avoided. The problem is that it is very difficult to design a highly absorbent, broad-band absorber good for low frequencies using a flat lining. This is why the anechoic wedge was developed. With enough depth and with an optimum impedance, a flat lining will absorb sound reasonably well. However, a wedge design would be better if the wedges were aligned with the flow as shown in figure 15(a). This is the approach used by Boeing in their 9- by 9-Foot Wind Tunnel. Because of the large surface area, the parallel-wedge lining would have high flow loss. However, it may be possible to combine the wedge-lining concept with a porous cover plate mounted at the wedge tips in order to protect the wedges from the flow, as shown in figure 15(a). This is very similar to the classic acoustic lining and porous cover plate, with the exception that the absorbent material is not in blanket form but in wedge shape. Figure 15(a) shows parallel wedges, but with a porous cover plate. It may be advantageous to alternate the wedge orientation and improve sound absorption as is commonly done in anechoic rooms. Five-foot-deep wedges would result in a test section 70×110 in cross section as illustrated in figure 15(b).

With the enhanced wall lining, the microphone/source spacing could be identical to that for an open jet. The microphones would be in the flow, but that is often the case with an open jet. One difficulty is that the flow noise on the microphone could cause the effective background noise to increase in certain frequency ranges. However, with large, noisy rotorcraft or V/STOL models, wind noise (unlike fan-drive noise, to be discussed) would not likely be a problem. The directional response of the microphones would be omnidirectional at the low- to mid-frequencies of interest on most tests, even with the microphones streamwise. All the problems of sound propagation through an open-jet shear layer would be avoided with this design.

The estimated maximum airspeed of a 70×110 test section with porous walls and a double acoustic-vane row is approximately 100 knots. Relative to the existing 80×120, the loss in airspeed due to the acoustic vanes is approximately offset by the increased airspeed due to a smaller test section.

Acoustically Transparent Wall

There may be an alternative to the simple enhanced wall lining. As discussed above, a closed-jet wall lining would probably require a porous protective interface at the lining. Going one step further, it may be possible to design a porous layer to replace the open-jet shear layer; i.e., the porous layer would separate the flow field from the anechoic room. Bauer (ref. 27) described an acoustically transparent wall that was designed to replace the hard wall of a wind tunnel test section (or open-jet shear layer) and allow the measurement of model noise outside the test section. That novel concept is based on the premise that a test section which contains the airflow with a minimum of leakage, yet allows the sound waves to pass unhindered, would have all the aerodynamic advantages of a closed-jet test section and all the acoustic advantages of an open-jet test section. That may be impossible to achieve perfectly, but a compromise between a little leakage and a little sound attenuation might be acceptable. This is not to say that the open-jet shear-layer problems would be avoided. The transition from the jet to the quiescent air would refract and scatter sound. However, that transition would be thin and would match closely the thin shear-layer refraction model (ref. 11). Furthermore, the acoustic scattering from turbulence might be weaker than it is in the comparatively thick shear layer of an open jet.

The wall evaluated by Bauer was a composite of 34% open-area perforated metal plate covered by a sintered-metal mesh that gave a specific flow resistance, R_f, of 100 mks rayls. An acoustic transmission loss of approximately 1 dB was measured over a frequency range from 63 to 16 kHz; i.e., 1 dB of the sound was reflected or absorbed by the wall. Using the method of Pierce (ref. 28), the transmission loss, R_{TL}, of a porous wall can be calculated:

$$R_{TL} = 10 \log ((1+1/2(R_f/\rho c)\cos\theta)^2) \quad \text{for } \omega >> R_f/m_{b\ell} \tag{2}$$

Thus, the acoustic transmission loss of a porous layer depends only on specific flow resistance at the layer, the characteristic impedance of air (ρc), and the angle of incidence relative to the normal vector. Using Bauer's porous-wall specific flow resistance, 100 mks rayls, equation (2) gives a transmission loss of 1 dB, which is what Bauer measured. Equation 2 is valid for frequencies greater that 6 Hz, assuming a porous material weight, $m_{b\ell}$, of 2.5 kg/m^2 (8.2 oz/ft^2). Note that equation (2) indicates that a porous layer would have even less transmission loss for sound incident at acute angles to the wall ($\theta > 0°$).

From reference 28, it can be shown that the ratio of acoustic energy absorbed by the porous layer to the acoustic energy transmitted, in terms of acoustic pressure squared, is as follows:

$$p_a^2/p_t^2 = R_f/(\rho c/\cos\theta) \tag{3}$$

For normal incidence sound impacting a porous layer with a specific flow resistance of 100 mks rayls, the absorbed acoustic energy would be 25% of the transmitted acoustic energy according to equation (3). And since the incident acoustic energy equals the sum of the transmitted, absorbed, and reflected acoustic energy, it follows that the reflected acoustic energy is 0.7% of the incident acoustic energy for these conditions. In terms of decibels, if the observed sound was 100 dB without a porous layer between the source and observer, the interposition of the porous layer would reduce the observed sound to 99 dB and create a reflected sound level of 79 dB on the source side of the layer, assuming equal path lengths from the source to observer locations. Under these conditions, the amount of energy reflected would have little impact on acoustic measurements inside the test section unless the reflection reached a quiet region—say, one that was well shielded from the direct sound field. So, as with an open-jet design, microphones could be placed inside or outside the flow to capture the radiated model noise with little concern about sound attenuation (outside) or reflections (inside).

Aerodynamically, the porous wall evaluated by Bauer performed well when substituted for a 38-in. length of hard wall in a small wind tunnel. The wind tunnel flow was contained with some leakage; the boundary layer on the wall was comparable to that on a hard wall. However, Bauer found that the boundary-layer interaction with the holes in the porous layer generated high-frequency noise ($f > 2$ kHz). At 8 kHz, that noise was 10 dB above the noise of the equivalent open jet. To deal with that, he recommended the use of suction to maintain a laminar boundary layer. There may also be ways to tailor the porous-layer hole geometry to minimize the flow noise.

At low frequencies (f < 500 Hz), the porous wall was much quieter than the equivalent open jet, since open jets have high levels of low-frequency noise due to shear layer fluctuations.

An acoustic insert in the 80×120, with acoustically transparent walls, could be built larger than 30×60 and still achieve the goal of 200 knots airspeed. By eliminating the shear layer, the flow losses of the test section reduce considerably. Liu and Mount (ref. 29) measured drag from a porous composite sheet bonded to woven wire that is similar in many respects to Bauer's porous-wall material. Their data show that the porous material had approximately 20% more drag than a smooth flat plate. With that information, the wind tunnel losses were estimated using the method described in the appendix A. The maximum test section speed of a 40×80 test section with porous wall is estimated to be 209 knots, whereas the top speed with the 30×60 open jet was estimated to be 197 knots (fig. 12). The acoustic vane loss was included. A 40×80 test section would be ideal for many models because they could be tested in the existing 40- by 80-Foot Wind Tunnel or in the aeroacoustic 40×80 insert, depending on test goals and schedules. Figures 16(a)-16(c) show a 40×80 test section with porous walls connecting an inlet nozzle and diffuser in the 80- by 120-Foot Wind Tunnel. Naturally, a smaller test section could be constructed using the porous wall concept if tradeoff studies showed that a large space outside the jet was more important than a large space inside the jet.

The structural framework needed to support the porous wall is not shown in figures 16(a)-16(c). The design of such a framework would be a challenge since the structure must be small or acoustically absorbent, yet robust enough to support the walls and airloads induced by the model. Furthermore, the floor would have to support personnel and equipment. It may be desirable, as Bauer recommended, to reduce the pressure in the volume surrounding the test section to control the boundary-layer development.

Another big advantage of the porous wall is that the flow in the test section would be much smoother than in an open jet. As discussed above, open-jet wind tunnels are notorious for poor flow quality due to the vortices and turbulence in the shear layer. Without the shear layer, the flow disturbances on the models and on the microphones would be greatly reduced in the test section; recirculation flow outside the test section would be eliminated; and the wall boundary layer would be larger than that on smooth walls, but the effect on most tests would be negligible. In fact, it is possible that a porous-wall facility could prove satisfactory for many aerodynamic studies. If the porous-walls could be protected from downwash and jet blast from V/STOL models, it might be possible to leave the insert in the 80×120 for aerodynamic tests, and only remove it for studies of models sized for the original 80×120 test section.

In addition to the acoustic and aerodynamic advantages cited above, a wind tunnel with acoustically transparent walls would not require a collector—an expensive item. However, the savings would be offset by the necessity to support the fragile porous wall over a long length.

The primary risk associated with the acoustically transparent wall is that the development of the concept is in its infancy. Bauer tested only one, small porous wall under one acoustic condition. Leakage was noted but not measured, pressure differentials were small and not variable as would be expected in a test section with a high-lift model, and vibrations were small due to the small size of the panel. Being a lightweight structure, the porous wall is fragile and could not easily be used as an insert in a large facility. Sound propagation through the porous wall and boundary layer would be refracted and distorted to some extent. The support framework would have to be acoustically nonobtrusive for the acoustic frequencies of interest. Nevertheless, development of the concept may lead to a viable design that would eliminate the numerous drawbacks of the open-jet wind tunnel.

PART 4 – AN ACOUSTIC VANE ROW TO CONTROL BACKGROUND NOISE

Each of the designs discussed above will require a duct silencer to attenuate the fan-drive noise entering the test section. Following are the requirements and a conceptual design for that acoustic vane set.

Background Noise

Existing– The background noise in the 80- by 120-Foot Wind Tunnel test section is dominated by the fan-drive noise. For their size, the fans are relatively quiet because of their low tip speed (377 ft/s) and improved inflow. However, The fans are located relatively close to the test section, being downstream and around the 45° corner connecting the 80×120 leg and the 40×80 circuit. See figure 1(b). Each of six 12.2-m diameter fans has 15 rotor blades and 23 stator blades, a number chosen for minimal modal propagation. The fans are operated with variable blade pitch and variable rotation speed up to a maximum speed of 180 rpm. The maximum sound power (ref. 30) of the fan-drive system is approximately 150 dB re 10^{-12} W. (The acoustical power is only 0.3% of the mechanical power of the fans, which is 135,000 hp).

Figure 17 shows estimated sound-pressure levels in the existing 80×120 test section at 96 knots airspeed (prior to installation of the acoustic lining—fig. 2), which is close to the top speed of the wind tunnel. The data were acquired with a model in the test section that generated extraneous noise which was removed from the spectrum.

Therefore, the spectrum may not be the true noise floor of the facility. The peak level was 104 dB in the 40 Hz third-octave band. That frequency band contains the fundamental harmonic of fan-blade-passage frequency, which is 45 Hz. The noise at the second harmonic (90 Hz) was 102 dB in the 80 Hz third-octave band.

Goal– Ideally, the background noise in the test hall should be at least 10 dB below the aircraft model noise at all frequencies. Many of the high powered models will generate noise levels above 120 dB. However, it is anticipated that models with noise control features will generate noise levels below 95-100 dB. Therefore, a goal of 85 dB maximum background noise out of flow in all third-octave bands of interest for a 200 knots test section speed would allow quality testing of all but very quiet models. Reducing the peak noise at 45 Hz to 85 dB means that the background noise above 200 Hz would be below 80 dB because of the spectrum roll-off with frequency (fig. 17). These levels are similar to the background noise levels in the test hall of DNW, which is 60-70 dB (above 200 Hz) at 155 knots or, by extrapolation using a noise variation (acoustic pressure squared) proportional to airspeed (or fan speed) to the 5.5 power, 66-76 dB at 200 knots test-section speed. The goal for the NASA Langley 14- by 22-Foot Wind Tunnel is 60-70 dB out of flow at 120 knots and, by extrapolation, 72-82 dB at 200 knots test-section speed (refs. 9 and 10), which is comparable to the goal for the 80×120.

Fan-Drive Silencers

To achieve the goal of 85-dB background noise at top speed of the facility, the projected peak background noise of 104 dB at 45 Hz must be attenuated 19 dB. That high level of attenuation at such a low frequency will require large sound-absorbent splitters or vanes in the duct between the test section and turning vanes (vane set 4) upstream of the fans. Soderman (refs. 31 and 32) performed parametric studies of several silencer designs including fiberglass-filled and resonant-cavity vanes that might be appropriate for this application. If the splitters are large, say 1.5 to 3.0 ft thick, the open passage must be of comparable size to prevent excessive pressure losses. In other words, the blockage must be 50% or less. If the open passages are that large, the medium- and high-frequency sound would be able to pass through the silencer with little attenuation. Thus, a second row of vanes is required that are aligned to block the line of sight of the preceding vane row. This is the method used in the NAL Transonic Wind Tunnel near Tokyo (refs. 33 and 34).

The splitters in the NAL Transonic Wind Tunnel have the geometry shown on figure 18. There are six rows of vanes . Counting from right to left (upstream to downstream), the first two rows are identical and offset to block the line of sight streamwise. Similarly, rows 3 and 4 are identical and offset, as are rows 5 and 6. The large splitters in rows 1 and 2 each have a 5.0-m chord, a 0.9-m thickness, and 2.0-m spacing center-to-center. The reported attenuation (refs. 33 and 34) is shown in figure 19(a) in terms of the cumulative attenuation. That is, the lower curve represents the attenuation of vane rows 1 and 2. The middle curve represents the attenuation of rows 1 through 4, and the upper curve gives the total attenuation of all six rows. Clearly, the larger vanes of rows 1 and 2 provided the most attenuation.

Figure 19(b) shows the estimated noise in the existing 80×120 with and without the double vane row. Although the peak attenuation is around 44 dB at 500 Hz, the attenuation at 63 Hz is only 11 dB. Thus, the desired attenuation of 19 dB at 45 Hz cannot be achieved with those vanes alone. Four vane rows would achieve that design goal, but that many vanes in the diffuser is probably impractical. It is recommended, therefore, that a double row of acoustic vanes be installed between the test section and vane set 4, which separates the 40×80 and 80×120 circuits, as shown in figures 13(a)-13(c). Those vanes would provide the required attenuation above 100 Hz and would have about 11 dB attenuation at 45 Hz, or 8 dB short of the goal. This shortcoming would affect full-scale helicopter noise studies primarily. However, it is estimated that typical helicopter models would generate enough low-frequency noise to overcome the fan-noise intrusion of 93 dB at 45 Hz. If this assumption proves to be incorrect, it would be necessary to lengthen the vanes or otherwise improve their low-frequency absorption as part of model scale testing and development.

Another method for improving the low-frequency attenuation of fan-drive noise would be to acoustically treat vane set 3. Vane set 3 closes off the 40×80 leg during operation of the 80×120, as shown in figure 13(a), and creates a wall which faces the fan drive. The low-frequency fan noise propagating upstream will diffract around vane set 5 and strike vane set 3, an effect documented by Soderman and Hoglund (ref. 35) in another wind tunnel. In that study, it was found that wall treatment in the corners of a wind tunnel was effective at absorbing low- to mid-frequency sound since that sound diffracted around the corner vanes. Acoustic treatment could be quite effective depending on the allowable depth of treatment.

Early in the study, it was hoped that one of the acoustic vane rows could be designed to replace vane set 4. Those vanes would then be permanent, so as to serve the double function of noise control and flow control. Only one vane row would have to be removed for operation of the original 80×120 closed test section. The difficulty with replacing the existing vane set 4 with an acoustic vane set is that the geometries are considerably different. The present vane set 4 is made up of seven flat baffles with a 6-in. thickness and 30-ft chord. During 40- by 80-Foot Wind Tunnel operation, the vanes are rotated and interlocked to form a wall blocking off the 80×120 leg. But, if the vanes had to attenuate sound, they would have to be thicker and closer together, as described

above, and would not fold together neatly to form a wall. The problem is illustrated in figure 20 which shows a 50% blockage vane set made up of 32-ft long vanes, 3.3-ft thick on 6.6-ft centers. When rotated to block off the 80×120 leg, the vanes must overlap each other. This creates an irregular surface that would generate turbulence upstream of the drive fans. Fairing that surface smooth would be difficult and expensive. Therefore, the acoustic vane rows would have to be placed upstream of the existing vane set 4 as shown in figures 13(a)-13(c).

It is unlikely that one or both acoustic vane rows shown in figures 13(a)-13(c) could remain in the wind tunnel during aerodynamic testing in the 80×120 test section (even with the open-jet nozzle, collector, and diffuser removed) because of high flow losses. Using the methods of the following section and appendix A, the top speed of the existing 80×120 test section would drop from 108 knots to approximately 83 knots with the introduction of one acoustic vane row and to approximately 72 knots with the introduction of a second vane row. Speed reductions such as these are unacceptable for most aerodynamic testing in the 80×120 test section. There is one exception to this: with the enhanced wall lining option, the speed reduction from the acoustic vanes would be offset by the speed increase from the 20% area reduction created by the lining. It is likely that the enhanced lining and the vane set could be left in the wind tunnel permanently.

Acoustic Vane Row Pressure Loss

The pressure loss for the two acoustic vane rows of figures 13(a)-13(c) can be estimated using the method of Mechel (ref. 36) modified by the results of Dudley et al. (ref. 37) and Soderman (ref. 38). Mechel developed an empirical prediction method for the normalized pressure loss of a vane set as follows:

$$\Delta p/q_1 = \eta_1(b/h)/(1 + (b/h)) + \eta_2\, \ell(2h) + \eta_3\, ((b/h)/(1 + (b/h)))^2 \qquad (4)$$

$$\Delta p/q_o = (q_1/q_o)/(\Delta p/q_1) \qquad (5)$$

where $\eta_1 = 0.05$ loss factor for vane nose

$\eta_2 = 0.0025$ loss factor for channel section (perforated)

$\eta_3 = 0.6$ loss factor for boattails with 6° wall angle

Dudley's (ref. 37) experimental results for parallel-baffle flow loss, however, indicated that Mechel's loss factors were in error for the type of baffles considered here. Specifically, Mechel's channel-flow loss is somewhat low, and the boattail loss is much too high. If the loss factors are changed to the following values, Mechel's empirical prediction and Dudley's data agree:

$\eta_1 = 0.05$ (no change)

$\eta_2 = 0.003$

$\eta_3 = 0.33$

Using the above loss factors in equations (4) and (5), we can evaluate the pressure drop from various acoustic vane geometries. And, the test-section flow speed reduction due to the vane rows can be computed using the method described in the appendix A. Consider the following vane-row geometry:

$2b$	= 1 m	vane thickness
$2h$	= 1 m	gap between vanes for 50% duct blockage
ℓ	= 4 m	channel length from aft end of nose to start of boattail

The computed pressure loss normalized by the local dynamic pressure (or loss coefficient), $\Delta p/q_1$, is 0.12. Assuming for the moment that the second vane row adds a loss coefficient of 0.12 without any interaction effects, the computed loss coefficient for two vane rows is 0.24.

PART 5 – MISCELLANEOUS COMPONENTS, AERO LOADS, AND LOGISTICS

Microphone Support Strut Design

The design of the microphone support struts outside of the flow is relatively unimportant, the only criterion being that the strut cross section be smaller than the smallest acoustic wavelength of interest. If this is not possible, the struts can be wrapped with sound-absorbent material. The microphone should be cantilevered forward of the main support strut (ref. 39). In many cases, a traversing microphone system is more desirable than fixed microphones for accurate studies of noise directivity.

The design of struts for in-flow microphones is more difficult because of the conflicting requirements for strength and rigidity versus low flow noise and minimal reflections. These requirements are complicated if the strut spans an open-jet shear layer.

(Struts can be cantilevered from the collector or nozzle, but those regions are usually avoided because of flow noise and reflections.) Any strut in the highly turbulent shear layer will experience unsteady loads resulting in radiated noise and possibly severe vibrations at the strut tip. The strut vibrations can be minimized by using a

fairing around the main strut in the shear layer as shown in figure 21. By sealing the gap between fairing and strut with a rubber seal, the vibration path can be broken.

The flow noise from the strut and fairing can be minimized by proper design. The cross sections should be aerodynamically clean; NACA airfoils are preferred over commercial airfoil tubing with blunt trailing edges which allow flow separation (ref. 40).

Vortex-street shedding can be a problem in certain Reynolds number regimes, but can be defeated by employing boundary-layer trips on the leading edge. To minimize reflections, the struts should have as small a chord as possible for the required rigidity, especially near the microphone. Airfoils will reflect sound waves comparable to or smaller than the chord (ref. 41). In most cases, a tapered strut can be employed to provide the strength low on the strut where needed. Figure 21 shows a design for low airspeeds which employs polyurethane foam glued to an airfoil-shaped spar. The foam absorbs sound and minimizes reflections.

Typical flow noise levels experienced by microphones on a typical strut in a closed wind tunnel were reported by Soderman (ref. 40) to be around 88 dB at 4-kHz third-octave band for flow speeds of 153 knots. That level can vary, of course, depending on strut design and turbulence levels in the flow. Noiseux (refs. 42 and 43) reported flow noise levels 13 dB below the values of reference 40 on a streamlined, tapered strut in a low-turbulent flow.

Insert Component Size

The practicality of a removable open-jet insert for the 80- by 120-Foot Wind Tunnel depends to a large extent on the material expense and the logistics of storing, installing, and removing the insert. It is beyond the scope of this study to investigate material costs or installation details. However, an estimate has been made of the quantity and sizes of the various components required and is shown below. From this, costs and installation procedures can be estimated. Only the basic surface panels have been itemized; support structure has not. The acoustic vanes, for example, will require structural support through the 80×120 floor to the ground. In fact, the acoustic vanes could be mounted on jacks and lowered out of the 80×120 if necessary for higher-speed operation. Flat acoustic linings will be needed for the collector and nozzle and certain wall areas.

The weights of the components have not been calculated. However, it is likely that the existing 80×120 structure would have to be reinforced just to carry the acoustic wedges, not to mention the other large components.

30×60 Open Jet

	Approximate area, ft^2 (each)
NOZZLE	
Side wall	11,700
Top or bottom	17,000
COLLECTOR	
Side wall	3000
Top or bottom	4400
DIFFUSER	
West wall	6400
East wall	2600
Ceiling or floor	7700
WEDGES	
Number of wedges	9500
Size	5-ft high by 2- × 4-ft base area
Wall area covered	190-ft by width or height of 80×120
ACOUSTIC VANES	
Number of vanes: 17	
Chord: 16 ft	
Span: 40 ft	

Aerodynamic Loads on Existing Structure

Increasing the 80×120 test-section velocity from 100 knots to the expected 200 knots with the 30×60 open-jet insert would increase the aerodynamic loads on the wind tunnel walls upstream of the fan drive because pressures in the open jet will control pressures in the surrounding duct. Under normal operating conditions of the 80×120, static pressures upstream of the fan drive are below atmospheric pressure. Increasing the maximum velocity of the test section from 100 to 200 knots will decrease the wall static pressure by as much as a factor of four, and will thereby increase the wall loads by a factor of four. In some areas, such as the inlet and much of the contraction, the load increases are not expected to be a problem because the governing loads are, and will continue to be, determined by atmospheric winds or seismic conditions. In other areas, such as the part of the circuit between the downstream end of the contraction and vane set 4, an increase in static operating loads by a factor or four will require structural strengthening of the wall cladding and superstructure. It should also be noted that the open-jet configuration will increase the unsteady aerodynamic loads on the structure because of the unsteady characteristics of the open jet, as previously discussed.

Recommended Model Scale Testing

As is stated many times in this report, the design development will require model scale testing to resolve many of the aerodynamic and acoustic uncertainties. Much could be accomplished with component testers and a complete model incorporating the proposed inserts with the 80×120 inlet, test section, 45° corner, and fan drive. The model could be simplified by using a single fan to represent the six-fan drive. The scale should be as large as practicable: 1/15th scale has been used successfully for 80×120 test-section flow and fan-performance studies (refs. 44-46), and the model wind tunnel is existing. The scale models would be necessary for the following studies of the chosen design concept:

1. Measure the separated flow regions downstream of the insert diffuser and the resulting velocity distortion at the fan drive. Modify the acoustic vane set or vane set 4 to control the flow field.

2. Measure insert pressure losses and resulting mass flow at the fan drive to evaluate stall margin of the fans.

3. Document velocity magnitudes and distribution (steady and unsteady) in insert test section as a function of operating condition. Modify the nozzle and collector as appropriate.

4. Identify and control shear layer induced flow instabilities of the open jet.

Evaluate any coupling of flow instabilities with acoustic modes of the 80×120 wind tunnel.

5. Measure acoustic reflections from the open-jet nozzle and collector. Control reflections with acoustic linings as necessary.

6. Evaluate acoustic absorption of wall linings on the 80×120 walls both analytically and experimentally.

Existing aerodynamic codes, including 2-D and 3-D panel codes, and new CFD codes would be used to support the experimental studies and aid the design process.

CONCLUDING REMARKS

An engineering feasibility study was made of aeroacoustic inserts for the 80- by 120-Foot Wind Tunnel at NASA Ames Research Center. The advantages and disadvantages of several designs were analyzed. The maximum airspeed of the the test section was the key factor in the design. To achieve airspeeds of 200 and 150 knots with the necessary acoustic quality, the design process led to a 30- × 60-ft and 40- × 80-ft test section, respectively. A 100-knots test section would best be achieved with an enhanced lining in the existing closed test section. All designs would require installation of a double acoustic vane row between the test section and fan-drive section. The conceptual designs are described below as a function of maximum airspeed.

1. 200 knots: 30×60 open jet. This is the largest possible test section which would achieve a 200 knots maximum airspeed (approximately) and allow placement of microphones in the acoustic far-field of models sized for the test section. A nozzle, collector, and diffuser would be required. Acceptable flow quality and acoustic characteristics could be achieved. Quality acoustic measurements would be possible inside or outside the flow. Acoustic detection studies could be made far upstream. It may be possible, at low airspeeds, to measure noise at large distances through the large test section door openings on the east side. Careful scale-model testing will be required to control shear-layer induced resonances at high speeds. Flow-control features will be needed in the double vane row to control separated flow from the diffuser downstream end. That turbulent flow might otherwise adversely impact the fan drive downstream. Increased pressure losses will move the fan toward stall. Therefore, stall margin must be checked in scale model tests.

2. 150 knots: 40×80 open jet. This concept is similar to item 1 with the advantage that models sized for the 40- by 80-Foot Wind Tunnel (closed section) could be tested in the aeroacoustic insert. The disadvantage is that the distance from the shear layer to the surrounding walls would be restricted such that, in many directions, microphones could not be placed in the acoustic far-field of large models. On the other hand, there would be more room inside the jet for inflow acoustic measurements.

3. 100 knots: 80×120 with improved acoustic lining. This is the simplest modification considered: only an improved wall lining would be installed in the existing wind tunnel. However, because of the need for good low-frequency absorption, acoustic wedges would probably be required. The resulting flow losses and speed loss would be severe unless a porous wall were placed over the wedges. The microphones would have to be installed in the flow. With a porous interface, the top speed would be close to the present top speed of the 80- by 120-Foot Wind Tunnel, (approximately 100 knots), since the speed loss due to increased flow losses from the lining and acoustic vane set would be offset by the increased speed in a 20% smaller cross section, assuming a 5-ft deep lining on all four walls.

4. 100-200 knots: Acoustically transparent walls. Acoustically transparent walls, which contain the airflow, could be incorporated with a nozzle and diffuser to achieve almost any airspeed. The transparent walls would separate the flow field from an anechoic room surrounding the test section. Model noise could be measured inside or outside the jet. This design would eliminate the unsteady flow from the open-jet shear layer, although acoustic refraction and scattering by the shear layer would occur. Both the aerodynamic and acoustic quality of the facility would be enhanced. The open-jet collector would be eliminated, although a complex structure would be required to hold the transparent wall without interfering with the acoustic field. Because of the uncertainty of successfully developing this unproven design, both from a

structural and aeroacoustic standpoint, this design must be considered a remote possibility.

The conclusion of this study is that an aeroacoustic insert in the Ames 80- by 120-Foot Wind Tunnel is technically feasible. The open-jet designs would be very difficult to implement due to the size of the necessary components. However, they could allow virtually anechoic acoustic studies of large-helicopter models, jets, and V/STOL aircraft models in simulated flight at speeds up to 200 knots. Model scale studies would be required to resolve several problems such as (a) flow separation at the diffuser downstream end that could feed highly turbulent flow into the fan section, (b) attenuation of fan noise with acceptable flow loss and adequate fan stall margin, and (c) open-jet resonances which could perturb the flow and impose large unsteady loads on the wind tunnel structure. Those are the highest risk items in the development. Any of them could limit the top speed of the facility to something less that 200 knots, or restrict the size of the test section. Successful development of acoustically transparent walls, though not necessary for three of the concepts, could lead to an aeroacoustic facility superior in many ways to the classical open- or closed-jet wind tunnel. The closed jet with enhanced wall lining design would be relatively easy to implement compared to the other concepts, but would only allow a 100 knots maximum airspeed, which is the operational airspeed of the current 80- by 120-Foot Wind Tunnel.

The large size of the open-jet inserts would make installation and removal of the components time-consuming. Each of the nozzle, collector, and diffuser wall panels have an area of several thousand square feet. Support structure would be required, not only to support the insert components, but to reinforce the existing structure because of higher pressure loads that would be up to four times the present loads. Just installing 9500 acoustic wedges would take a significant effort. Consequently, scheduling of the existing 80×120 aerodynamic test section and scheduling of the aeroacoustic test section would likely be made on an annual or longer basis. In contrast, the enhanced wall lining design would likely be permanently installed; although the modifications are technically feasible, a cost estimate is necessary to evaluate the practicality of this project. The optimal design choice depends on the required maximum airspeed, which has yet to be determined.

Ames Research Center
National Aeronautics and Space Administration
Moffett Field, California 94035-1000
January 10, 1990

APPENDIX A

WIND TUNNEL PRESSURE LOSS AND POWER BALANCE EQUATIONS

Loss Coefficients

Idelchik (ref. 21) developed the following empirical equations for pressure loss in open jets and truncated diffusers.

$$h = \Delta p/(\rho U^2/2) \qquad (1)$$

where

- Δp = total pressure drop in test section
- ρ = fluid density
- U = average flow speed in test section

For the test section:

$$\eta_t = 0.0845\, \ell/D_h - 0.0053\, (\ell/D_h)^2 \qquad (2)$$

- η_t = test section loss coefficient
- D_h = hydraulic diameter = 4 A_t /Per
- A_t = area of test section nozzle
- Per = perimeter of nozzle = 2 (width + height)

For a 30- × 60-ft test section 120-ft long:

- ℓ = 120
- D_h = 40
- η_t = 0.2058

The above value of test section loss coefficient compares favorably with the DNW loss factor derived in Appendix B. For the wind tunnel performance calculations summarized in tables 3-7, the DNW open-jet loss coefficient was used.

For the truncated diffuser:

$$\eta_{diff} = (1+\sigma)\left[\frac{\lambda(1+2(\rho/D_h)\tan(\alpha/2))^2+1}{8\sin(\alpha/2)(1+2(\rho/D_h)\tan(\alpha/2))^2-1} + k_2\tan(\alpha/2)\tan^{1/4}(\alpha/2)\right] \times \left[1-\frac{1}{(1+2(\rho/D_h)\tan(\alpha/2))^2}\right]^2 + \left[\frac{1}{(1+2(\rho/D_h)\tan(\alpha/2))^2}-\frac{1}{n}\right]^2 \qquad (3)$$

where

- σ = $0.5 - 0.4545\, A_o/A_1$
- A_o = diffuser inlet area
- A_1 = diffuser exhaust area
- λ = duct friction coefficient
  - = $64/R_e$ ($R_e < 2000$)
  - = $0.1\,(1.46\,\delta + 100/R_e)^{0.25}$ ($R_e > 2000$)
- R_e = Reynold's number based on diameter
- δ = relative roughness = h/D_h
- h = typical height of roughness
- α = total diffuser angle (twice wall angle)
- k_2 = 6 (empirical constant)
- n = A_2/A_o
- A_2 = duct area downstream of diffuser truncation

For a 30- × 60-ft diffuser entrance, a 110-ft diffuser length, and an 8° total diffusion angle, the loss coefficient using the above equation is:

$$\eta_{diff} = 0.194$$

Loss coefficients for other wind tunnel components listed in tables 3-7 came from existing data and other empirical predictions.

Wind Tunnel Power Balance

The power output required by the wind tunnel fan system is equal to the sum of the flow power losses in each section of the wind tunnel including the power or kinetic energy of the flow as it exhausts from the nonreturn wind tunnel.

The power output by the fan is:

$$P = T_f\, U_f = \Delta p_f\, A_f\, U_f \qquad (4)$$

where

- T_f = fan thrust
- U_f = average velocity at the fan section
- Δp_f = pressure rise through the fan section
- A_f = cross sectional area of fans

The fan power is balanced by the sum of the power losses at each section.

$$P = \Sigma \Delta P_i \qquad (5)$$

The power loss at a typical duct section i is:

$$\Delta P_i = D_i U_i = \Delta p_i A_i U_i \qquad (6)$$

where

D_i = aerodynamic drag at section

A loss coefficient, η_i, can be defined as:

$$\eta_i = D_i / (A_i Q_i) = \Delta p_i / Q_i \qquad (7)$$

where

Q_i = dynamic pressure at the i^{th} section $= \rho U_i^2 / 2$

So

$$P = \Sigma \Delta P_i = \Sigma(\eta_i Q_i A_i U_i) = \Sigma(\eta_i \rho U_i^3 A_i / 2) \qquad (8)$$

And from conservation of mass in incompressible flow, $A_t U_t = A_i U_i$ where the subscript t refers to the test section.

Therefore

$$\Delta p_f = (\rho A_t^2 U_t^2 / 2) \Sigma (\eta_i / A_i^2) \qquad (9)$$

relates the fan pressure rise to the test section speed, given the appropriate areas and loss coefficients at each section. Additionally, the fan horsepower consumption is given by:

$$P_c = (\Delta p_f A_f U_f)/(550 \eta_f) \qquad (10)$$

where the fan efficiency, η_f, is approximately 0.88.

APPENDIX B

TEST SECTION PRESSURE LOSS OF DNW

Open-jet pressure losses can be computed from calibration data acquired at DNW and compiled in a report by the staff of DNW—Compilation of Calibration Data of the German-Dutch Wind Tunnel, MP-82.01, 13 March 1982. The computation is based on the relationship between fan power required and wind tunnel flow losses.

$$P = \Delta p_f A_f U_f \tag{1}$$

where

P = fan power output, N-m/s or W
Δp_f = fan pressure rise, N/m^2
A_f = cross sectional area of duct at fan, m^2
U_f = average airspeed at fan, m/s

From equation (9) in Appendix 1:

$$\Delta p_f = (\rho A_t^2 U_t^2 / 2)\, \Sigma\, (\eta_i / A_i^2) \tag{2}$$

where

A_t = cross-sectional area of test section, m^2
U_t = test section airspeed, m/s
η_i = loss coefficient of i^{th} circuit component
A_i = cross-sectional area of i^{th} duct section or component, m^2

Combining equations (1) and (2):

$$P = Q_t A_t U_t\, S\, (\eta_i (A_t/A_i)^2) \tag{3}$$

where

Q_t = dynamic pressure in the test section, N/m^2

Or, to separate the test section loss from the rest of the circuit losses,

$$P = Q_t A_t U_t (\eta_t + \Sigma\, (\eta_j A_t/A_j)^2) \tag{4}$$

where

$j = j^{th}$ circuit component. The summation in equation (4) excludes the contribution from the test section.

Solving for the test section loss factor,

$$\eta_t = P/(Q_t A_t U_t) - \Sigma(\eta_j (A_t/A_j)^2) \tag{5}$$

Assuming that the circuit losses given by the summation $\Sigma(\,)$ will not change whether the test section is configured as a closed or open jet, the difference in loss between an open and closed test section is given by:

$$\Delta\eta_t = (P/(Q_t A_t U_t))_o - (P/(Q_t A_t U_t))_c \tag{6}$$

where the subscripts o and c refer to an open or closed test section, respectively.

From plots of brake shaft power versus wind tunnel speed in the DNW calibration report, equation (6) can be solved for the DNW 8- by 6-m test section, which was calibrated as an open and closed test section. From figures 2.3 and 2.4 of that report, the following data were acquired.

Test Section	U_t, m/s	P, MW
8- × 6-m closed (unslotted walls)	98	8
8- × 6-m open jet	82	8

Using the above numbers in equation (6) along with the test section area of 48 m^2, we get $\Delta\eta = 0.493 - 0.289 = 0.204$. In reference 16, the 8- × 6-m closed test section and contraction loss coefficient based on tests of scaled components is given as $\eta_t = 0.028$. Again, assuming that that difference in DNW power consumption during open-jet and closed-jet test section operation is due primarily to changes in test section losses, it follows that the open-jet loss coefficient is:

$$\eta_{t\ \text{open jet}} = 0.028 + 0.204 = 0.232$$

This open-jet loss coefficient is reasonably close to the value of 0.206 computed using Idelchik's method as described in Appendix A. Since the proposed open jet designs in this report are geometrically similar to the DNW design, the loss factor of 0.232 will be used in the wind tunnel performance calculations.

REFERENCES

1. Mort, K.W.; Soderman, P.T.; and Meyn, L.A.: Optimum Full-Scale Subsonic Wind Tunnel. AIAA Paper 86-0732-CP, AIAA 14th Aero. Testing Conf., Mar. 1986.

2. Mort, K.W.; Soderman, P.T.; and Eckert, W.T.: Improving Large-Scale Testing Capability by Modifying the 40- by 80-Foot Wind Tunnel. J. Aircraft, vol. 16, no. 8, Aug. 1979, pp. 571-575.

3. Mort, K.W.; Engelbert, D.F.; and Dusterberry, J.C.: Status and Capabilities of the National Full Scale Facility—40- by 80-Foot Wind Tunnel Modification, AIAA Paper 82-0607, Mar. 1982.

4. Soderman, P.T.: Oblique Incidence Sound Absorption of Porous Materials Covered by Perforated Metal and Exposed to Tangential Airflow. Inter-Noise 82, vol. 2, May 1982, pp. 401-404.

5. Wilby, J.F.; and White, P.H.: An Analysis of Sound Absorbing Linings for the Interior of the NASA Ames 80- by 120-Foot Wind Tunnel. NASA CR-177396, 1985.

6. Penaranda, F.E.; and Freda, M.S., eds.: Aeronautical Facilities Catalogue—Volume 1: Wind Tunnels. NASA RP-1132, Jan. 1985.

7. Mort, K.W.; Kelly, M.W.; and Hickey, D.H.: The Rationale and Design Features for the 40- by 80-/80-by 120-Foot Wind Tunnel. AGARD CP-174, Paper 9, Oct. 1975.

8. Soderman, P.T.: A Comparison of Wind Tunnels Suitable for Rotorcraft Noise Studies. In Rotorcraft Noise. NASA CP-2234, 1982, pp. 45-62.

9. Hayden, R.E.; and Wilby, J.F.: Sources, Paths, and Concepts for Reduction of Noise in the Test Section of the NASA Langley 4 × 7 m Wind Tunnel. NASA CR-172446-1, 1984.

10. Yu, J.C.; and Abrahamson, A.L.: Acoustic Treatment of the NASA Langley 4- by 7-Meter Tunnel: A Feasibility Study. NASA TP-2563, Aug. 1986.

11. Amiet, R.K.: Correction of Open Jet Wind Tunnel Measurements for Shear Layer Refraction. AIAA Paper 75-532, Mar. 1975.

12. Ross, R.: Spectral Broadening Effects in Open Wind Tunnels in Relation to Noise Assessment. AIAA J., vol. 19, no. 5, May 1981, pp. 567-572.

13. Guedel, A.: Scattering of an Acoustic Field by a Free Jet Shear Layer. J. Sound and Vibration, vol. 100, no. 2, 1985, pp. 285-304.

14. Rebuffet, P.; and Guedel, A.: Tests on 8/100th Scale Model for the Definition of the Convergent and Collector of CEPRA 19 (Anechoic Open Jet Wind Tunnel). AIAA Paper 81-1989, AIAA 7th Aeroacoustics Conf., Oct. 1981.

15. Abramovich, G.N.: The Theory of Turbulent Jets. (Scripta Technica, transl.) The MIT Press, Cambridge, 1963.

16. Boxwell, D.A.; Schmitz, F.H.; Splettstoesser, W.R.; Schultz, K.J.; Lewy, S.; and Caplot, M.: A Comparison of the Acoustic and Aerodynamic Measurements of a Model Rotor Tested in Two Anechoic Wind Tunnels. NASA TM-88364 and USAAVSCOM TM 86-A-6, Nov. 1986.

17. Van Ditshuizen, J.C.A.; Courage, G.D.; Ross, R.; and Schultz, K.J.: Acoustic Capabilities of the German-Dutch Wind Tunnel DNW. AIAA Paper 83-0146, 21st Aerospace Sciences Conf., Jan. 1983.

18. Van Ditshuizen, J.C.A.; and Ross, R.: Aerodynamic and Aeroacoustic Design Aspects. Construction 1976-1980: Design Manufacturing Calibration of the German-Dutch Windtunnel (DNW), M. Seidel, ed., DNW, 1982, pp. 16-22.

19. Martin, R.M.; Brooks, T.F.; and Hoad, D.R.: Reduction of Background Noise Induced by Wind Tunnel Jet Exit Vanes. AIAA J., vol. 23, no. 10, Oct. 1985, pp. 1631-1632.

20. Applin, Z.T.: Modification To The NASA Langley 4- by 7-Meter Tunnel For Improved Rotorcraft Aerodynamics & Acoustics. AHS Natl. Specialists Meeting on Helicopter Testing Technology, Williamsburg, VA, Oct. 1984.

21. Idelchik, I.E. (A. Barouch, transl.): Handbook of Hydraulic Resistance. AEC-tr-6630, Atomic Energy Commission, 1966 (available from Dept. of Commerce, Springfield, VA).

22. Introduction to Design and Performance Data for Diffusers. ESDU 76027, Engineering Sciences Data Unit, London (England), Nov. 1976.

23. Schubauer, G.B.; and Spangenberg, W.G.: Effect of Screens in Wide-Angle Diffusers. NACA TN-1610, July 1948.

24. Rehbein, U.; and Hoffman, R.: Acoustic Liner in the Measurement Hall. Translation of "Schallabsorbierende Auskleidung in der Messhalle" translated from ref. 18, NASA TM-88437, June 1986.

25. Delany, M.E.; and Bazley, E.N.: The High Frequency Performance of Wedge-Lined Free Field Rooms. J. Sound and Vibration (1977), vol. 55, no. 2, pp 195-214.

26. Soderman, P.T. and Noble, S.C.: Directional Microphone Array for Acoustic Studies of Wind Tunnel Models. J. Aircraft, vol. 12, no. 3, Mar. 1975, pp. 168-173.

27. Bauer, A.B.: Acoustically Transparent Walls For Aeroacoustic Wind Tunnel Applications. AIAA Paper 76-92, AIAA 14th Aerospace Sciences Meeting, Washington D.C., Jan. 1976.

28. Pierce, A.D.: Acoustics–An Introduction to Its Physical Principles and Applications. McGraw-Hill Book Co., New York, 1981.

29. Liu, T-M.; and Mount, J.S.: Friction Drag Measurements for Acoustic Surfaces. AIAA Paper 83-1356, AIAA/SAE/ASME 19th Joint Propulsion Conf., Seattle, WN June 1983.

30. Soderman, P.T.; and Mort, K.W.: Aeroacoustic Characteristics of a Large, Variable-Pitch, Variable-Speed Fan System. Inter-Noise 83, Proceedings of 1983 International Conf. on Noise Control Engineering, vol. 1, July 1983, pp. 123-126.

31. Soderman, P.T.: A Study of Resonant-Cavity and Fiberglass-Filled Parallel Baffles as Duct Silencers. NASA TP 1970, April 1982.

32. Soderman, P.T.: Design and Performance of Resonant-Cavity Parallel Baffles for Duct Silencing. Noise Control Engineering, vol. 17, no. 1, 1981, pp.12-21.

33. Construction and Performance of NAL Two-Dimensional Transonic Wind Tunnel. NAL TR-647T, National Aerospace Laboratory (Tokyo), Feb. 1982.

34. Sakakibara, S.; Miwa, H.; Kayaba, S.; and Sato, M.: Investigation of the Components of the NAL High Reynolds Number Two-Dimensional Wind Tunnel, Part IV Design, Construction and Performance of the Exhaust Silencer. NASA TM-88513, Sept. 1986.

35. Soderman, P.T.; and Hoglund, L.E.: Wind-Tunnel Fan Noise Reduction Including Effects of Turning Vanes on Noise Propagation. AIAA Paper 79-0642, AIAA 5th Aeroacoustics Conf., Seattle, WN, Mar. 1979.

36. Mechel, F.P.: Design Criteria for Industrial Mufflers. Inter-Noise 75 Proceedings, Senai, Japan, 1975, pp. 751-760.

37. Dudley, M.R.; Unnever, G.; and Regan, D.R.: Two-Dimensional Wake Characteristics of Inlet Vanes for Open-Circuit Wind Tunnels. AIAA Paper 84-0604, Mar. 1984.

38. Soderman, P.T.; Unnever, G.; M.R. Dudley: Effect of Boattail Geometry on the Aeroacoustics of Parallel Baffles in Ducts. NASA TM-85981, July 1984.

39. Zaveri, K.: Influence of Tripods and Microphone Clips on the Frequency Response of Microphones. Bruel & Kjaer Technical Review no. 4 - 1985 (ISSN 007-2621), pp. 32-40.

40. Soderman, P.T.: Test-Section Noise of the Ames 7-by 10-Foot Wind Tunnel No. 1. NASA TM-X-73,134, May 1976.

41. Mueller, A.W.: A Comparison of the Three Methods Used to Obtain Acoustic Measurements for the NASA Flight Effects Program. NASA TM-81906, Oct. 1980.

42. Soderman, P.T.: Instrumentation and Techniques for Acoustic Research in Wind Tunnels. ICIASF '75 Record. Inter. Congress on Instrumentation in Aerospace Simulation Facilities, Sept. 1975, Ottawa, Canada, pp. 270-276.

43. Noiseux, D.U.; Noiseux, N.B.; and Kadman, Y.: Study of A Porous Microphone Sensor In An Aerofoil. NASA CR-137652, Mar. 1975.

44. Signor, D.B.; and Borst, H.V.: Aerodynamic Performance of Two Fifteen-Percent-Scale Wind-Tunnel Drive Fan Designs. AIAA Paper 86-0734, AIAA 14th Aero. Testing Conf., Mar. 1986.

45. van Aken, J.M.; and Scheller, N.M.: Experimental Investigation of Inlet Flow-Control Cascades for the NFAC 80- by 120-Foot Indraft Wind Tunnel. AIAA Paper 88-0054, AIAA 26th Aerospace Sciences Meeting, Reno, NV, Jan. 1988.

46. van Aken, J.M.; Ross, J.C.; and Zell, P.T.: Inlet Development for the NFAC 80- by 120-Foot Indraft Wind Tunnel, AIAA Paper 88-2528, AIAA 6th Applied Aerodynamics Conf. Williamsburg, VA, June 1988.

Table 1. Geometry and operation limits of one drive fan

	Rotor	Stator
Number of blades	15	23
Diameter	40 ft	40 ft
Hub-tip ratio	0.438	0.438
Root chord	4.02 ft	2.93 ft
Tip chord	2.96 ft	2.93 ft
Twist, root to tip	41.4°	5.3°
Maximum, rpm	180	0

Rotor/stator spacing = 9.02 ft (mid-chord to mid-chord)

Fan total pressure rise, $\Delta p = 55$ lb/ft^2

Table 2. Large-scale open-jet wind tunnels worldwide groups A and B (test section dimension > 12 ft)

Wind tunnel	Test section size, ft	Maximum velocity, knots
Langley 14- by 22-Foot	14.5 × 21.8	110
Langley 30- by 60- Foot	30 × 60	80
Boeing Vertol	20 × 20	100
McDonnell Douglas Mini-speed Tunnel	15 × 20	50
Canada NAE 15-foot	15 (diam)	45
Daimler-Benz 20-Foot	27 × 19	140
DNW	26 × 20	150
Ford of Europe #2	24 × 16	—
Japan Defense Agency	13 × 13	70
ONERA S1 Chalais-Meudon	26 ×52 (ellip)	96
RAE 24-Foot	23.7 (diam)	100
Swiss Federation Aircraft	16 × 23	130
Toulouse	13.9 (diam)	82
VW Climatic Wind Tunnel	30 × 20	100

Table 3. Estimated flow losses of the existing 80- by 120-Foot Wind Tunnel

% of total circuit loss	Local loss[a] coefficient	Normalized loss[b] coefficient	Component
10.2	2.00	0.10	Inlet
6.8	0.064	0.064	Test section
4.3	0.035	0.040	Vane set 4
15.9	0.130	0.150	Vane set 5
2.8	0.010	0.024	Fan stator
2.8	0.010	0.023	Fan swirl
0.9	0.017	0.009	Fan contraction, struts, diffuser
4.4	0.250	0.042	Vane set 6
26.2	1.73	0.248	Vane set 7
25.8			Kinetic energy at vane set 7
100.0		0.66	Total

Test section speed, knots	Fan pressure rise,[c] lb/ft^2	Fan power required,[d] hp
54.8	10	17871
67.1	15	32831
77.5	20	50547
95.0	25	70642
102.6	30	92861
109.6	35	117018
116.3	40	142968

[a] $\Delta p/q_i$

[b] $\Delta p/q_o$

[c] 55 maximum allowable

[d] 135000 maximum available

Table 4. Estimated flow losses of an open-jet insert with 30- by 60-foot nozzle, 120-foot test section, and collector/diffuser

% of total circuit loss	Local loss[a] coefficient	Normalized loss[b] coefficient	Component
1.1	2.00	0.000	Inlet
71.1	0.232	0.232	Test section
18.8	0.194	0.061	Diffuser
0.5	0.035	0.001	Vane set 4
1.7	0.130	0.006	Vane set 5
0.3	0.010	0.001	Fan stator
2.8	0.010	0.023	Fan swirl
0.1	0.017	0.000	Fan contraction, struts, diffuser
0.5	0.250	0.002	Vane set 6
2.8	1.73	0.009	Vane set 7
2.8			Kinetic energy at vane set 7
100.0		0.32	Total

Test section speed, knots	Fan pressure rise,[c] lb/ft^2	Fan power required,[d] hp
147.7	25	23175
161.8	30	30465
174.7	35	38390
186.8	40	46904
198.1	45	55968
208.9	50	65550
219.1	55	75625

[a] $\Delta p/q_i$

[b] $\Delta p/q_o$

[c] 55 maximum allowable

[d] 135000 maximum available

Table 5. Estimated flow losses of an open-jet insert with 30- by 60-foot nozzle, 150-ft test section, and collector/diffuser

% of total circuit loss	Local loss[a] coefficient	Normalized loss[b] coefficient	Component
0.9	2.00	0.000	Inlet
59.0	0.242	0.242	Test section
33.1	0.269	0.136	Diffuser
0.4	0.035	0.001	Vane set 4
1.4	0.130	0.006	Vane set 5
0.2	0.010	0.001	Fan stator
2.8	0.010	0.001	Fan swirl
0.1	0.017	0.000	Fan contraction, struts, diffuser
0.4	0.250	0.002	Vane set 6
2.2	1.73	0.009	Vane set 7
2.2			Kinetic energy at vane set 7
100		0.40	Total

Test section speed, knots	Fan pressure rise,[c] lb/ft^2	Fan power required,[d] hp
131.7	25	20663
144.2	30	27162
155.8	35	34228
166.6	40	41818
176.7	45	49899
186.2	50	58443
195.3	55	67425

[a] $\Delta p/q_i$

[b] $\Delta p/q_o$

[c] 55 maximum allowable

[d] 135000 maximum available

Table 6. Estimated flow losses of an open-jet insert with 30- by 60-foot nozzle, 120-foot test section, collector/diffuser, and double-row acoustic van set

% of total circuit loss	Local loss[a] coefficient	Normalized loss[b] coefficient	Component
0.9	2.00	0.000	Inlet
57.7	0.232	0.232	Test section
15.3	0.194	0.61	Diffuser
18.9	0.240	0.076	Acoustic vane set
0.4	0.035	0.001	Vane set 4
1.4	0.130	0.006	Vane set 5
0.2	0.010	0.001	Fan stator
2.8	0.010	0.001	Fan swirl
0.1	0.017	0.000	Fan contraction, struts, diffuser
0.4	0.250	0.002	Vane set 6
2.3	1.73	0.009	Vane set 7
2.3			Kinetic energy at vane set 7
100		0.39	Total

Test section speed, knots	Fan pressure rise,[c] lb/ft^2	Fan power required,[d] hp
133.0	25	20870
145.7	30	27435
157.4	35	34572
168.2	40	42239
178.4	45	50401
188.1	50	59031
197.3	55	68103

[a] $\Delta p/q_i$

[b] $\Delta p/q_o$

[c] 55 maximum allowable

[d] 135000 maximum available

Table 7. Estimated flow losses of an open-jet insert with 40- by 80-foot nozzle, 155-foot test section, collector/diffuser, and double-row acoustic van set

% of total circuit loss	Local loss[a] coefficient	Normalized loss[b] coefficient	Component
1.7	2.00	0.010	Inlet
35.5	0.232	0.232	Test section
23.3	0.219	0.152	Diffuser
25.5	0.240	0.167	Acoustic vane set
0.7	0.035	0.005	Vane set 4
2.7	0.130	0.018	Vane set 5
0.5	0.010	0.003	Fan stator
0.5	0.010	0.003	Fan swirl
0.2	0.017	0.001	Fan contraction, struts, diffuser
0.7	0.250	0.005	Vane set 6
4.4	1.73	0.029	Vane set 7
4.4			Kinetic energy at vane set 7
100		0.62	Total

Test section speed, knots	Fan pressure rise,[c] lb/ft^2	Fan power required,[d] hp
104.3	25	29089
114.2	30	38239
123.4	35	48186
131.9	40	58872
139.9	45	70249
147.5	50	82277
154.7	55	94922

[a] $\Delta p/q_i$

[b] $\Delta p/q_o$

[c] 55 maximum allowable

[d] 135000 maximum available

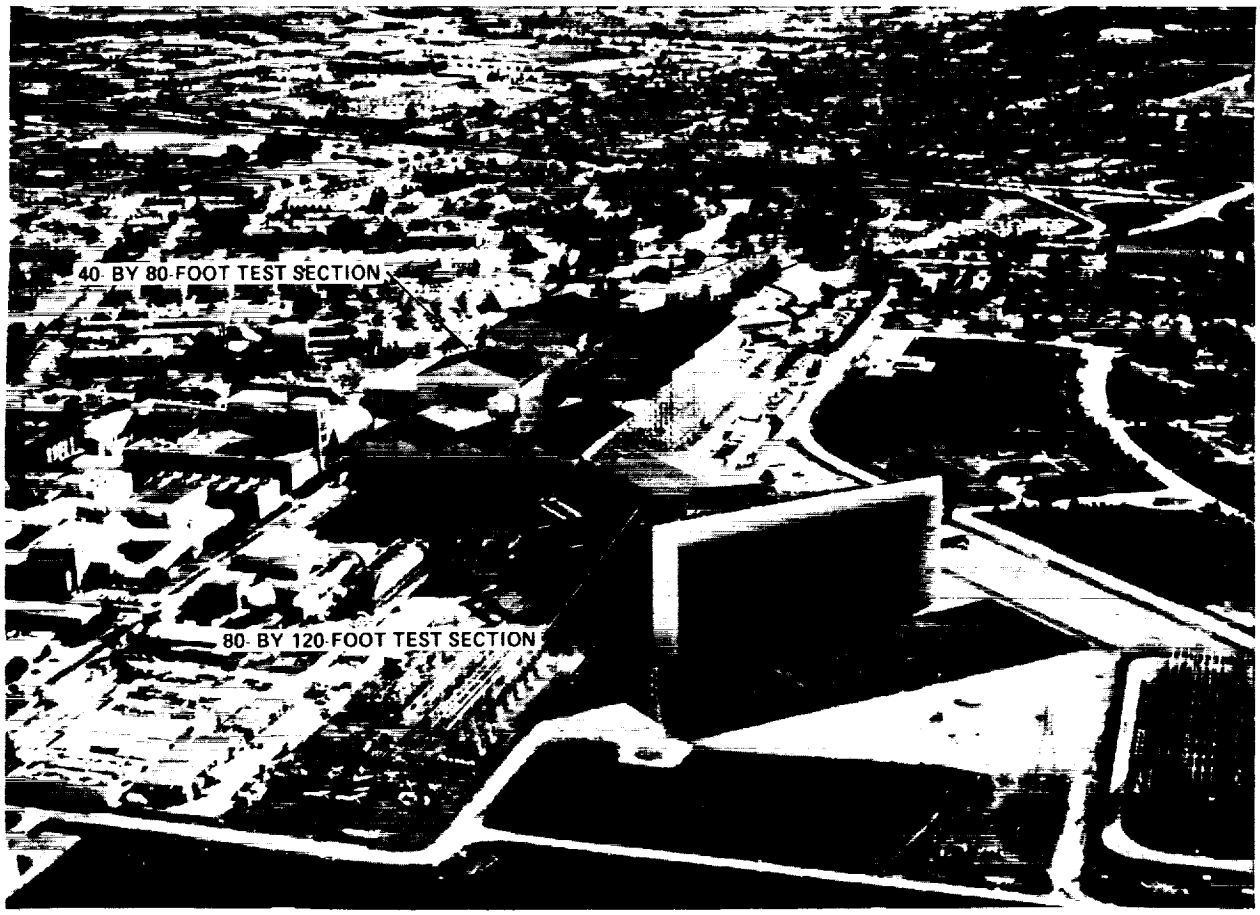

(a)

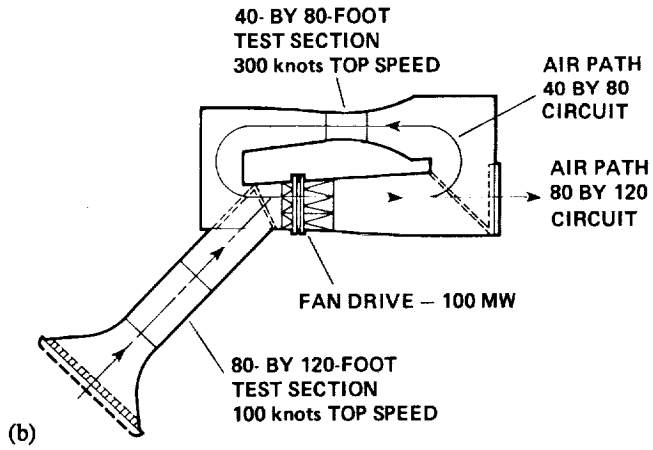

(b)

Figure 1.– NASA Ames 40- by 80-Foot/80- by 120-Foot Wind Tunnel. a) Photo of facility; b) plan view of circuit.

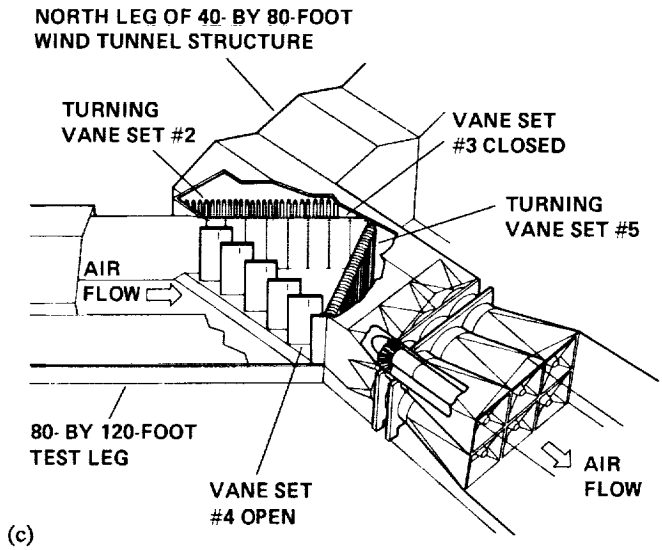

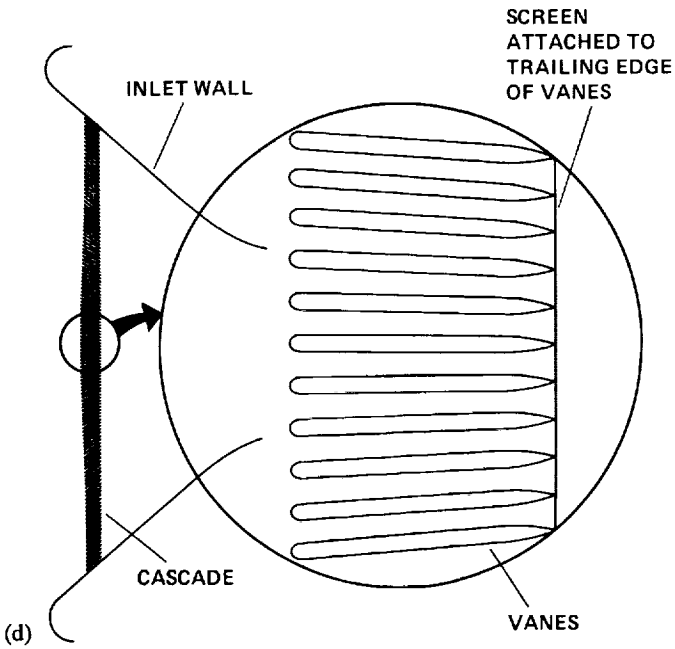

Figure 1.– Concluded. c) Vane arrangement for operation of the 80×120 circuit at the junction with the 40×80 circuit; d) 80×120 inlet vanes and anti-turbulence screen.

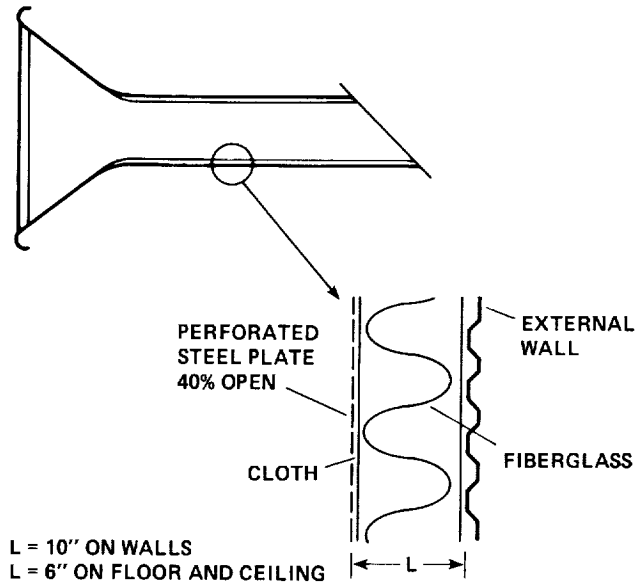

Figure 2.– Acoustic wall lining in the existing 80- × 120-ft test section.

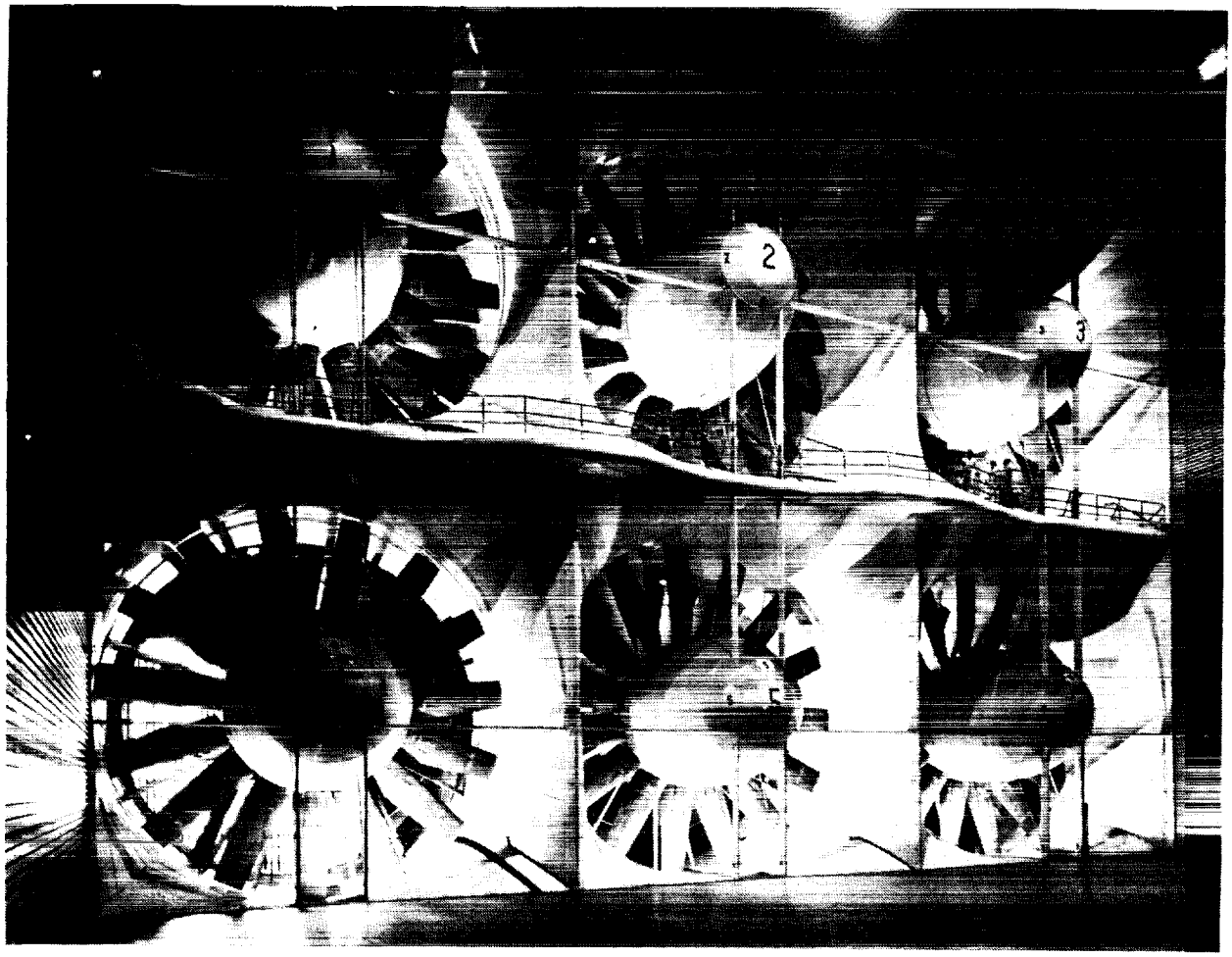

Figure 3.– Six 40-ft diameter fans in wind tunnel drive section.

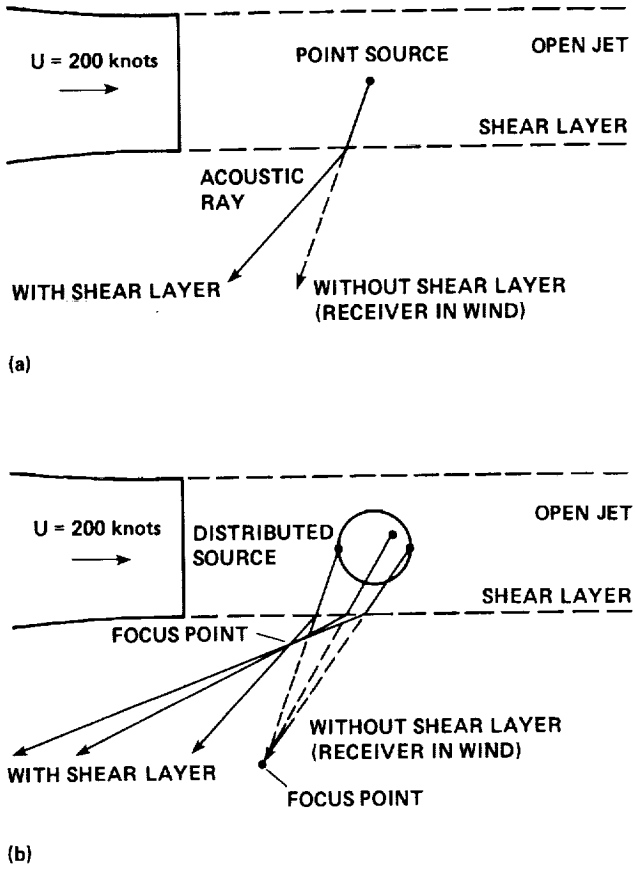

Figure 4.– Open-jet shear layer refraction which changes observed source directivity outside the jet; point-source and distributed-source propagation illustrated. a) Point noise source; b) distributed noise source.

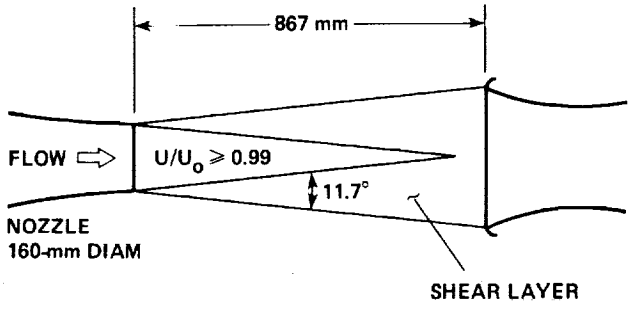

Figure 5.– Measured shear layer expansion in CEPRA 19 Anechoic Open Jet Wind Tunnel (circular jet) (from ref. 14).

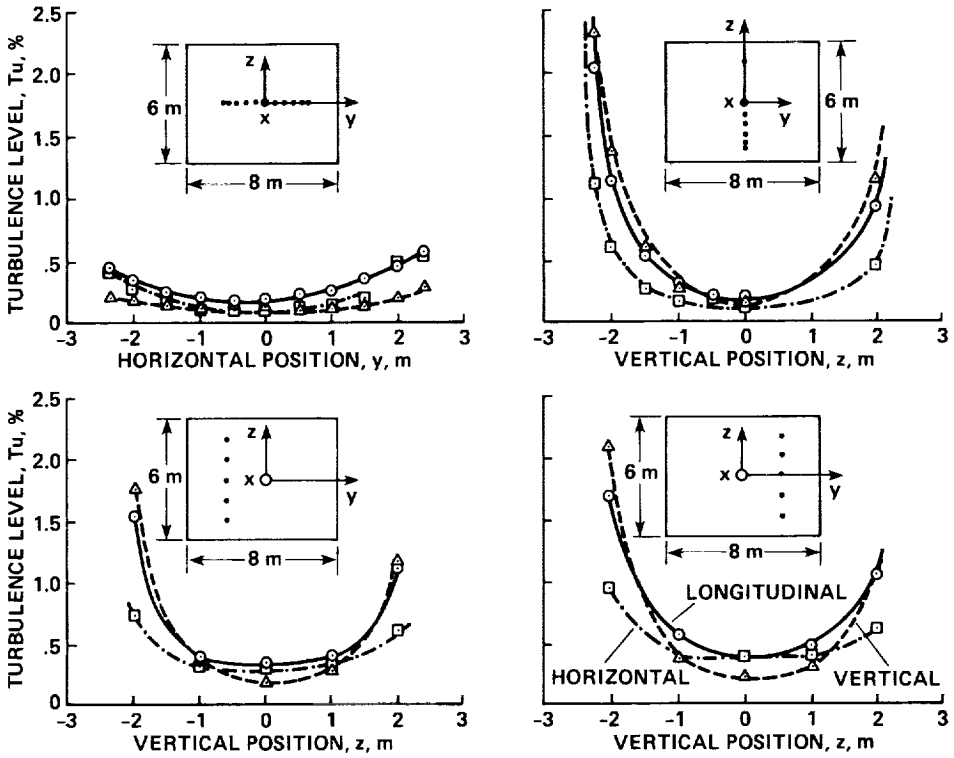

Figure 6.– Cross-stream distribution of turbulence in the DNW Wind Tunnel open jet (from ref. 17).

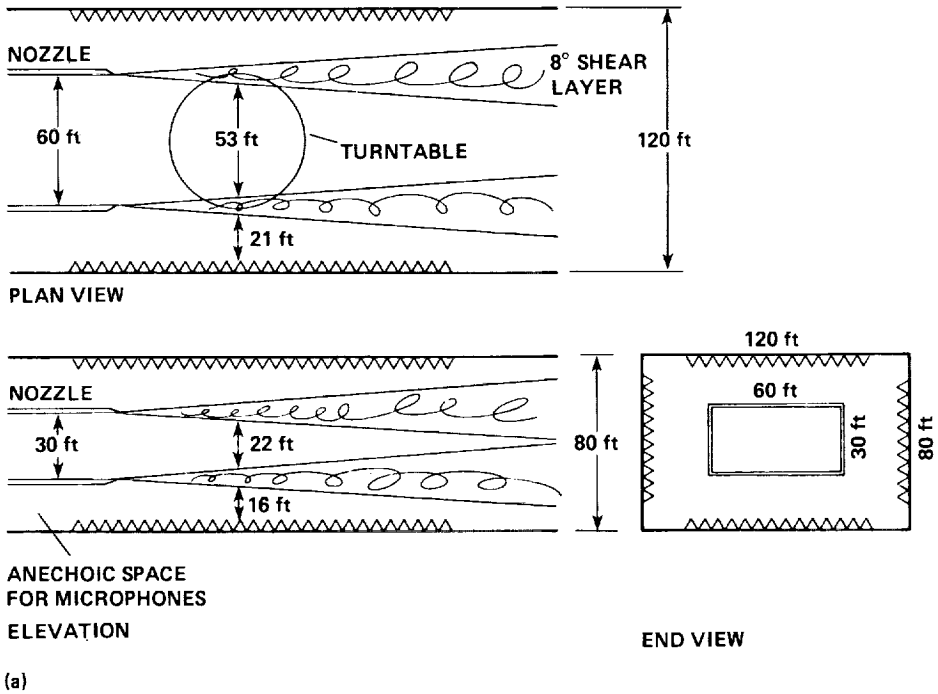

Figure 7.– Nozzle geometry and shear layer distribution. a) 30- × 60-ft nozzle.

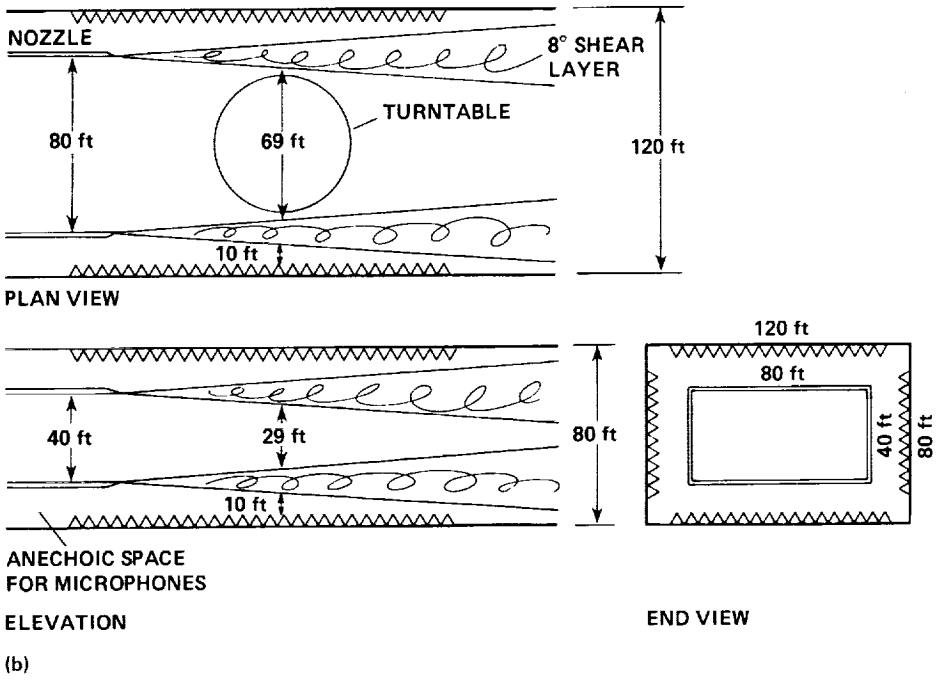

b) 40- × 80-ft nozzle.

Figure 7.– Concluded.

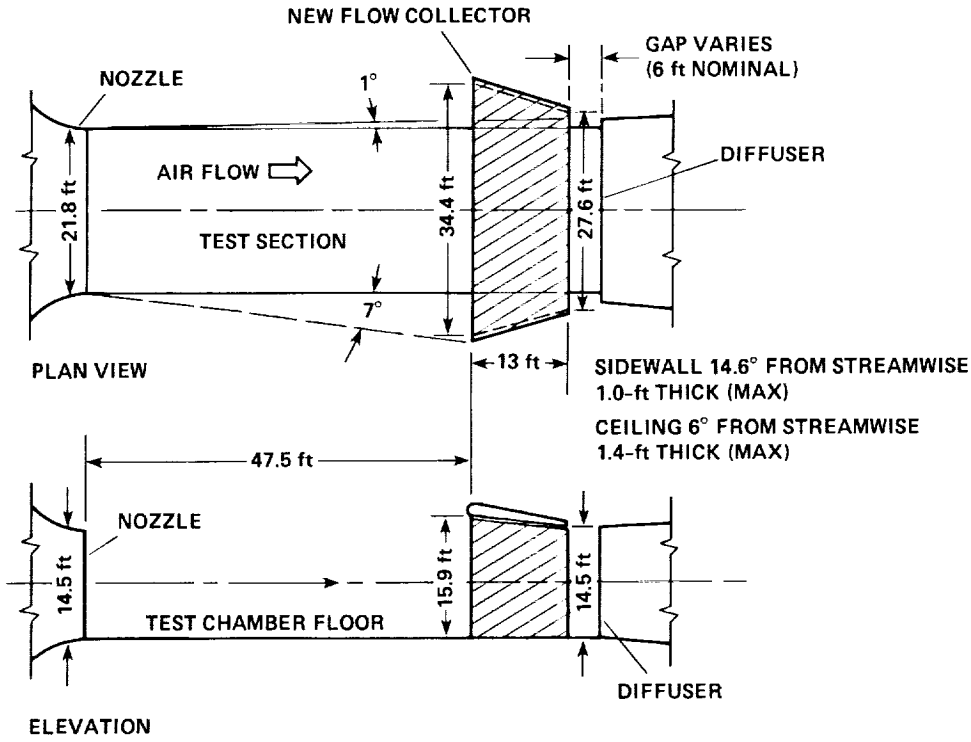

Figure 8.– Flow collector in NASA Langley 14- by 22-Foot Wind Tunnel.

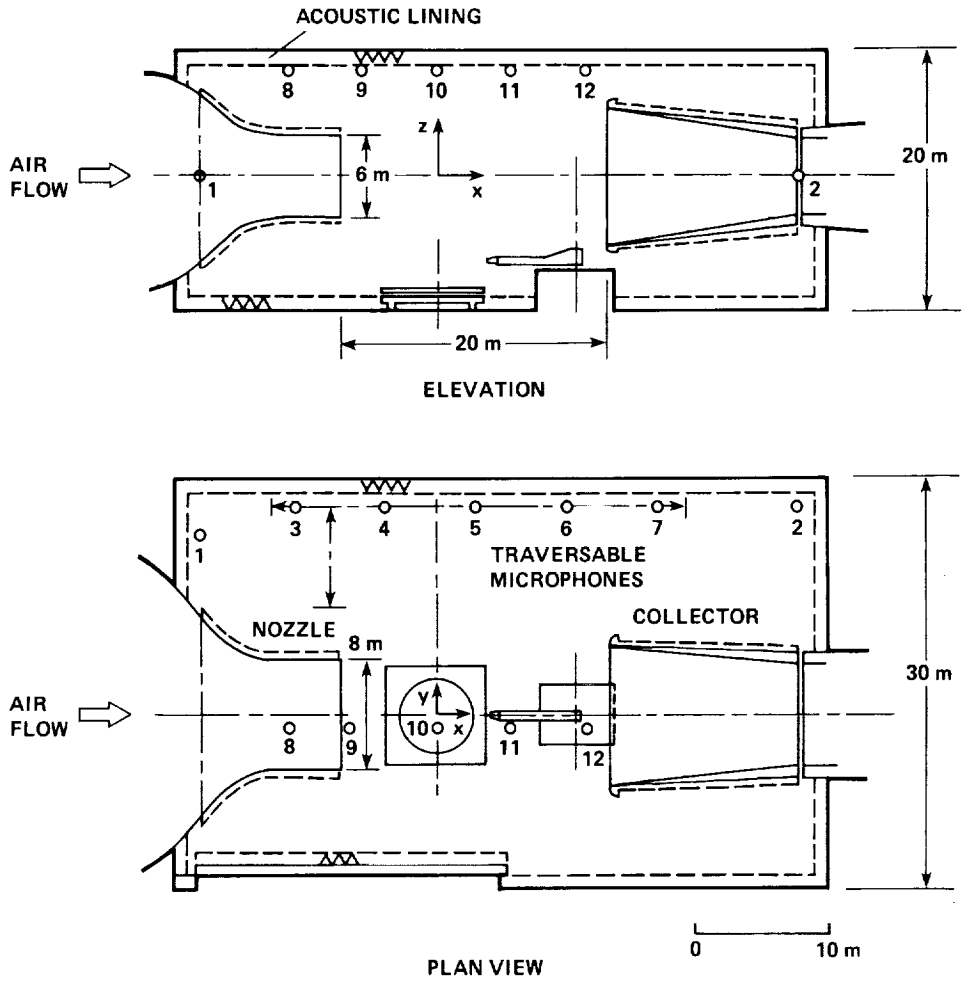

Figure 9.– DNW open-jet test section including nozzle and collector (from ref. 17).

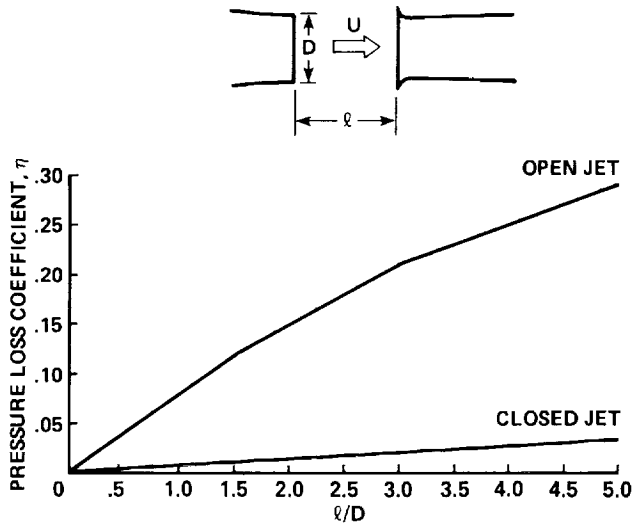

Figure 10.– Variation of loss coefficient with length of simple open or closed test section (from ref. 21).

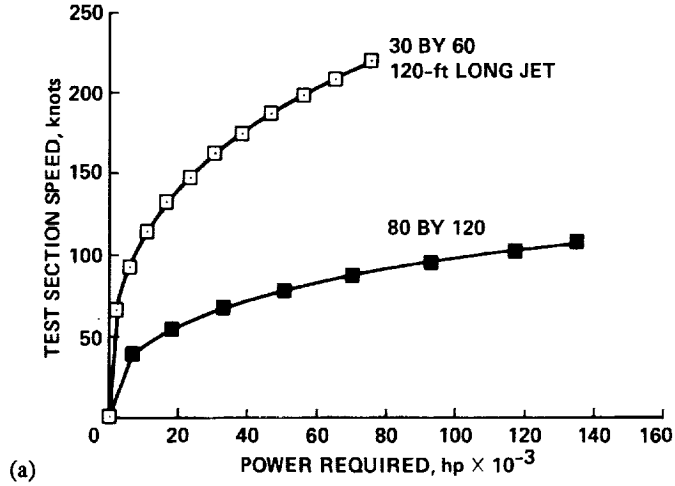

(a)

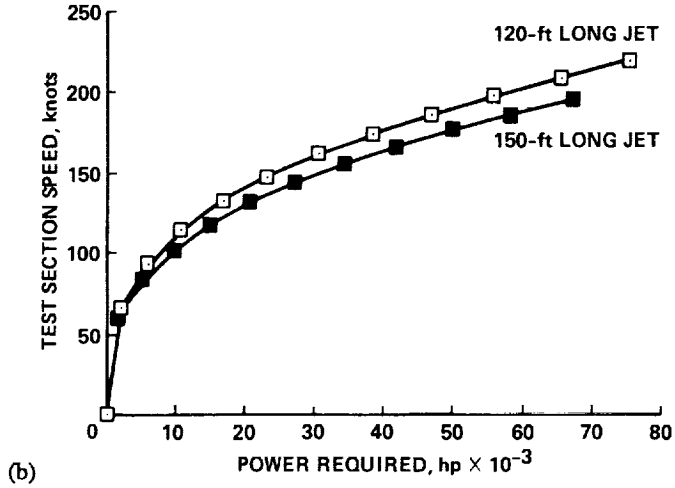

(b)

Figure 11.– Estimated test-section speed of the closed (existing) 80- × 120-ft and open 30- × 60-ft test sections. Acoustic vane loss not included. 80×120 max speed limited by power available. 30×60 max speed limited by max allowable fan pressure rise. a) Open jet and closed jet; b) comparison of 120- and 150-ft long 30- × 60-ft open jet.

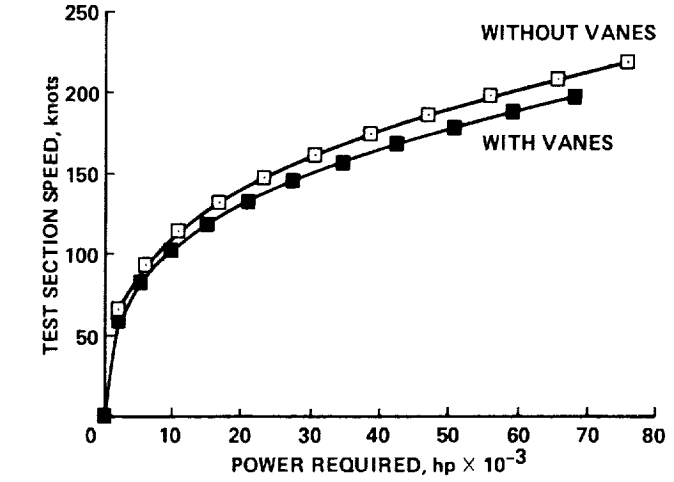

Figure 12.– Estimated test-section speed of the 30- × 60-ft open-jet (120-ft long) with and without a double-row acoustic vane set in the diffuser.

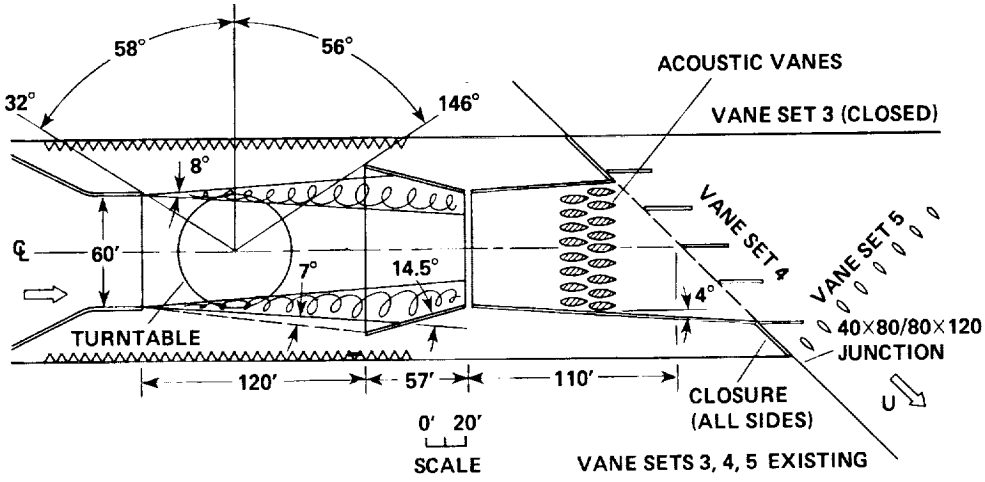

(a)

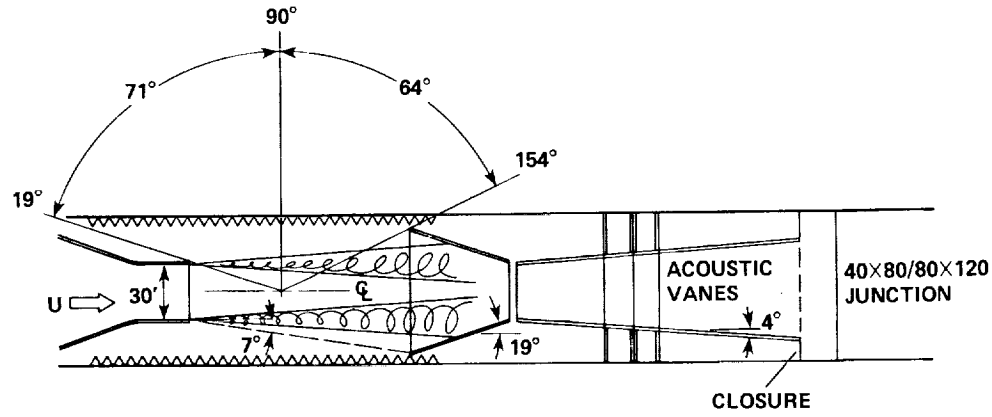

(b)

Figure 13.– 30- × 60-ft open jet with nozzle, collector, diffuser, and acoustic vanes. a) Plan view; b) elevation.

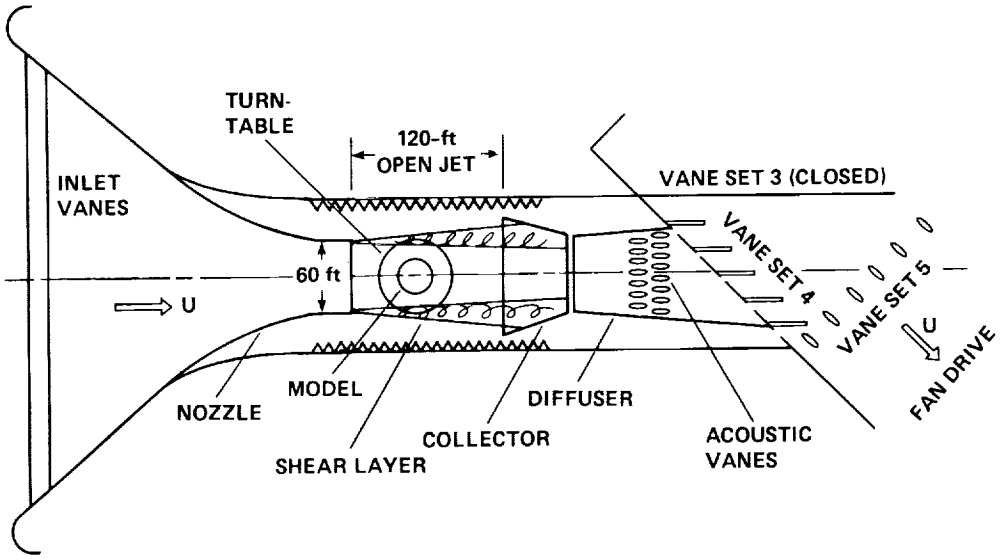

PLAN VIEW

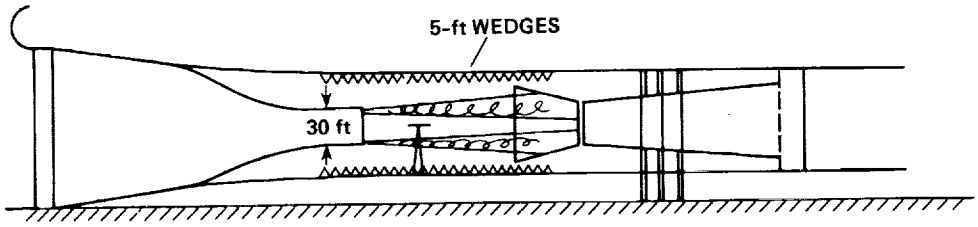

ELEVATION

(c)

c) Overall perspective.

Figure 13.– Concluded.

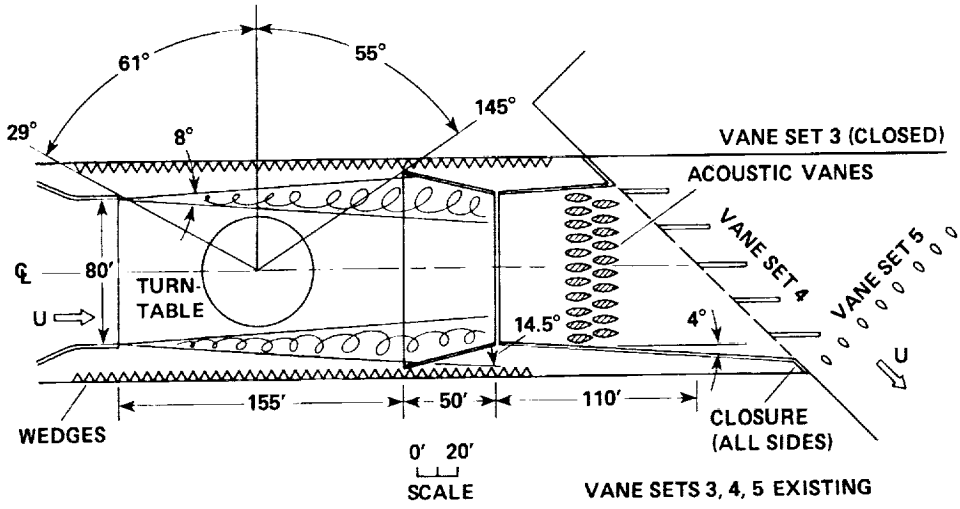

(a)

Figure 14.– 40- × 80-ft open jet with nozzle, collector, diffuser, and acoustic vanes. a) Plan view.

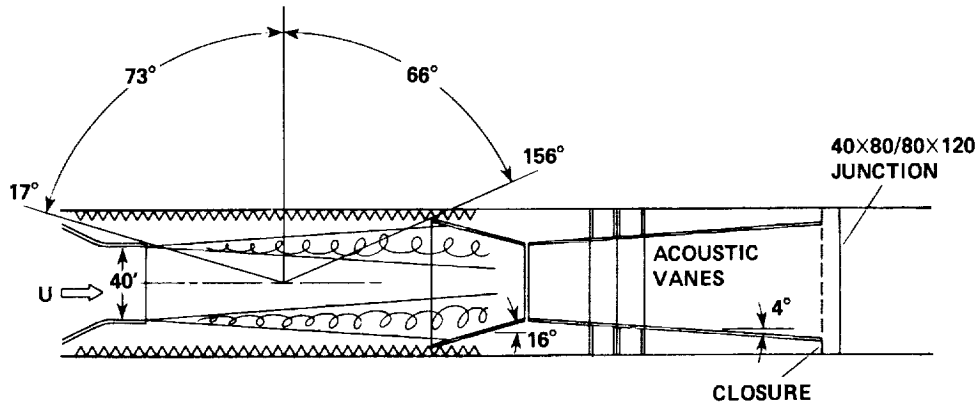

(b)

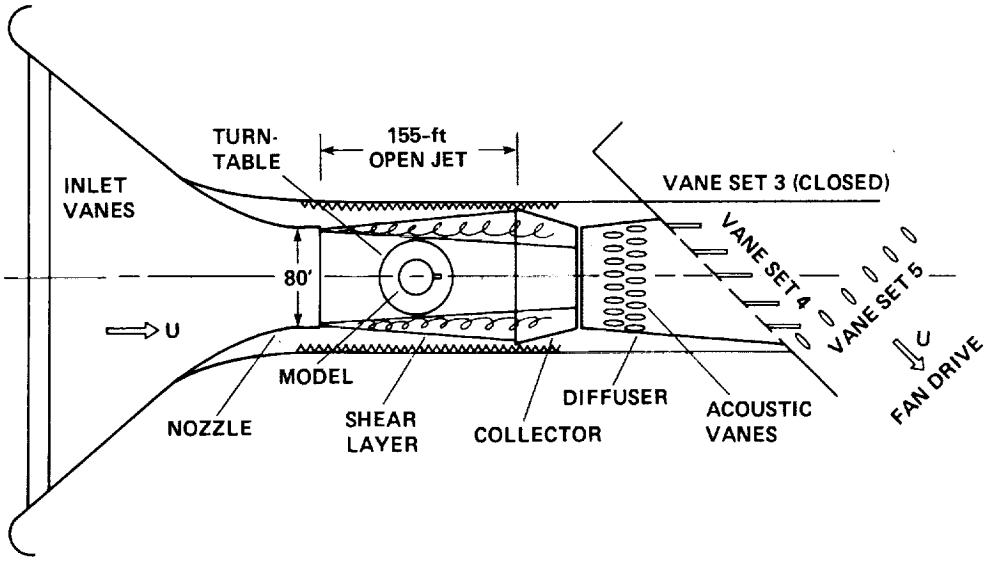

PLAN VIEW

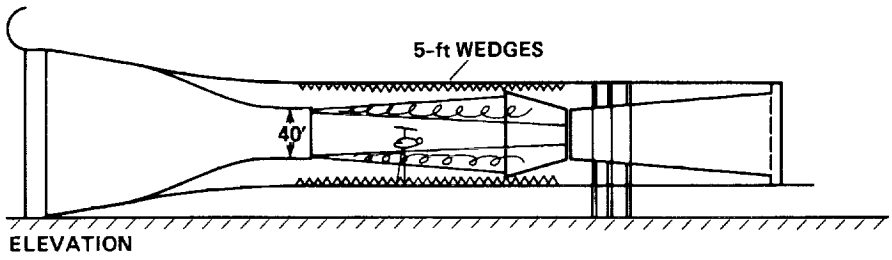

ELEVATION

(c)

Figure 14.– Concluded. b) Elevation; c) overall perspective.

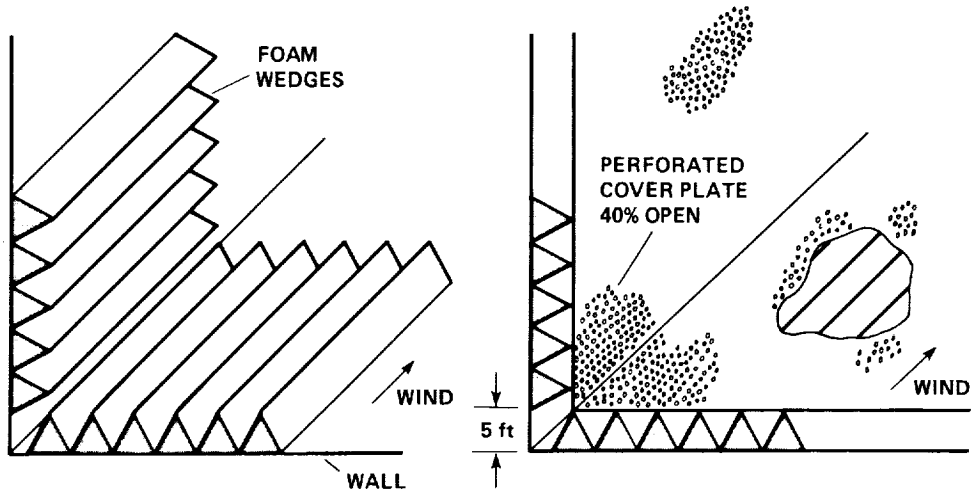

(a)

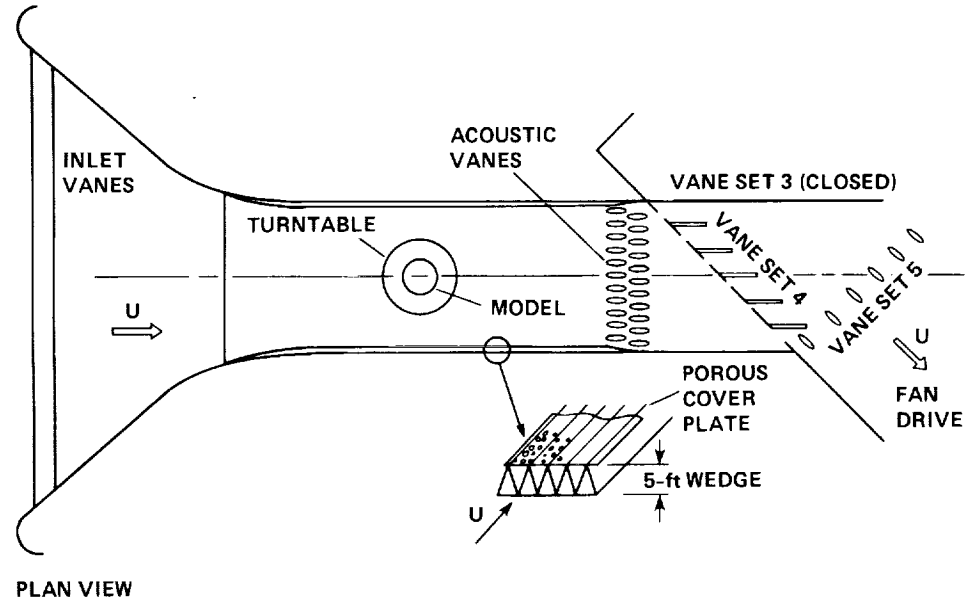

PLAN VIEW

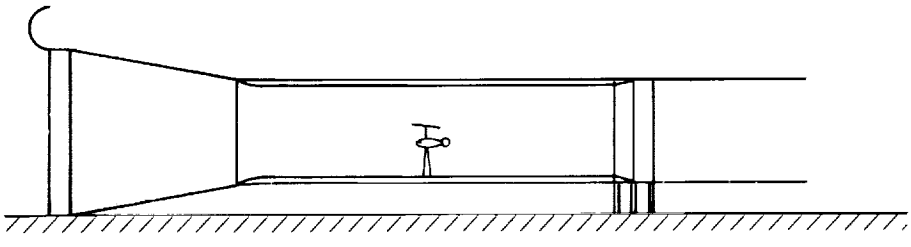

ELEVATION

(b)

Figure 15.– Two possible configurations of enhanced acoustic linings attached to the 80×120 walls, floor, and ceiling. a) Close view; b) far view.

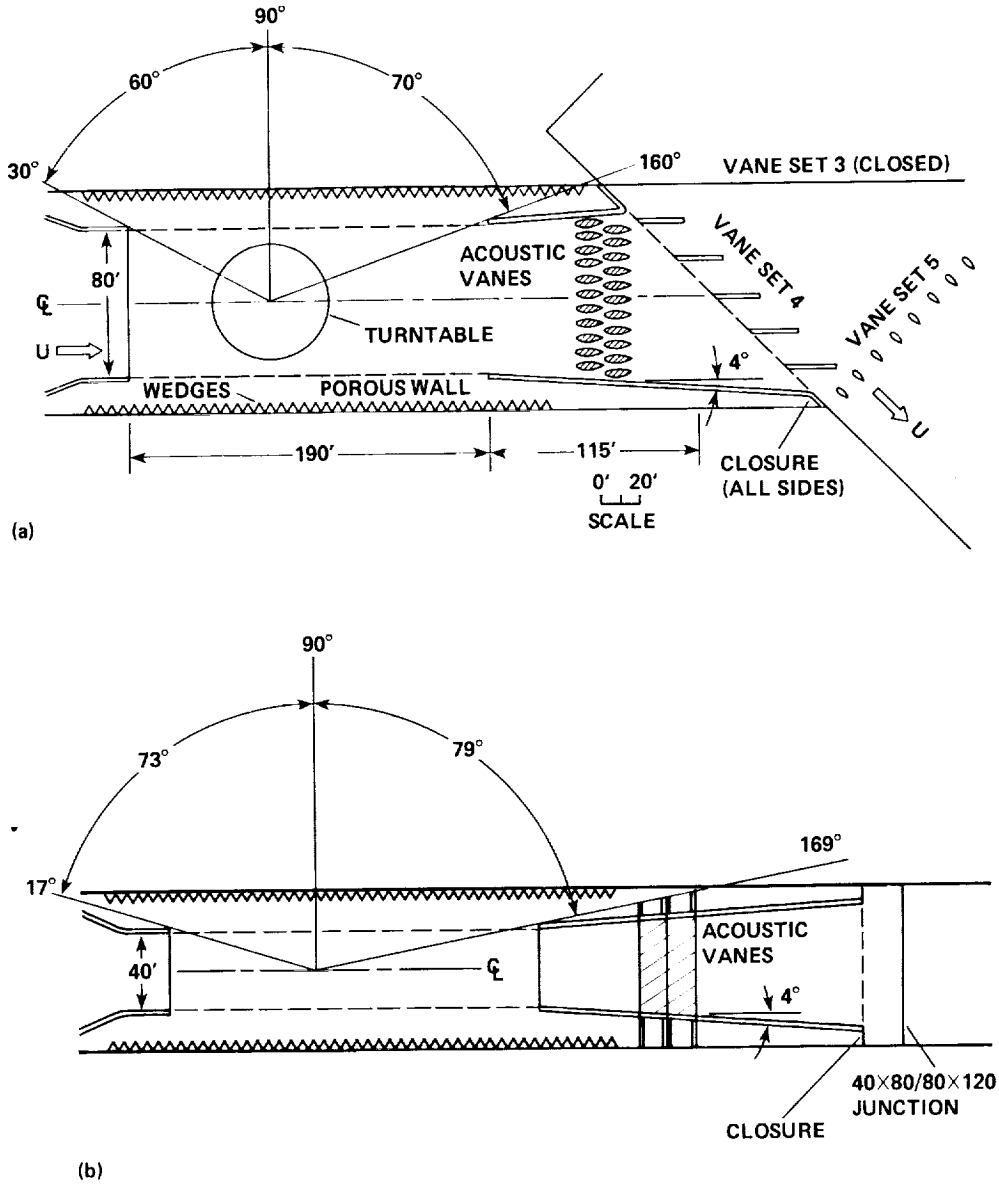

Figure 16.– 40- × 80-ft test section with acoustically transparent walls. a) Plan view; b) elevation.

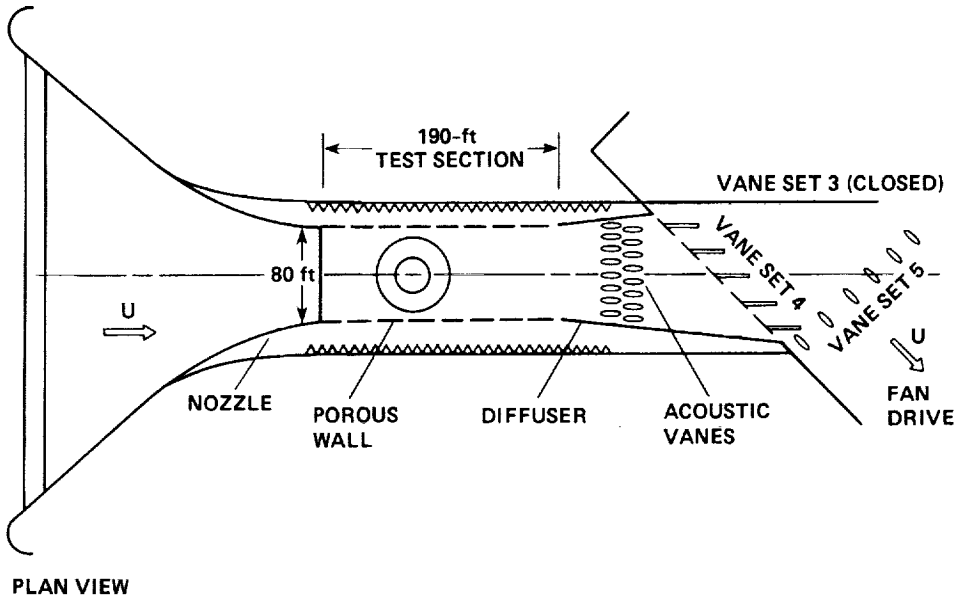

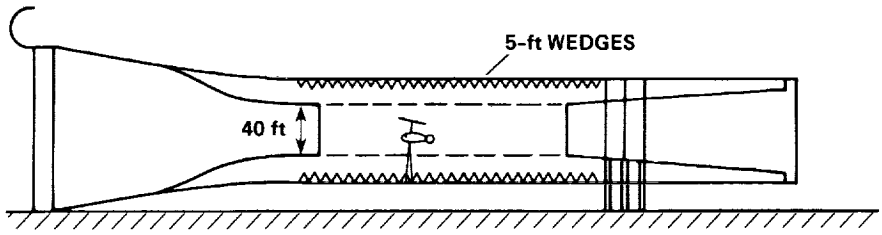

c) Overall perspective.

Figure 16.– Concluded.

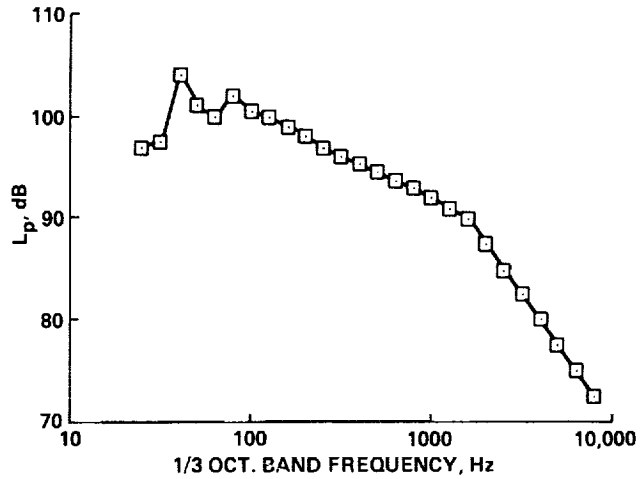

Figure 17.– Estimated background noise in the 80- by 120-Foot Wind Tunnel at 96 kts airspeed.

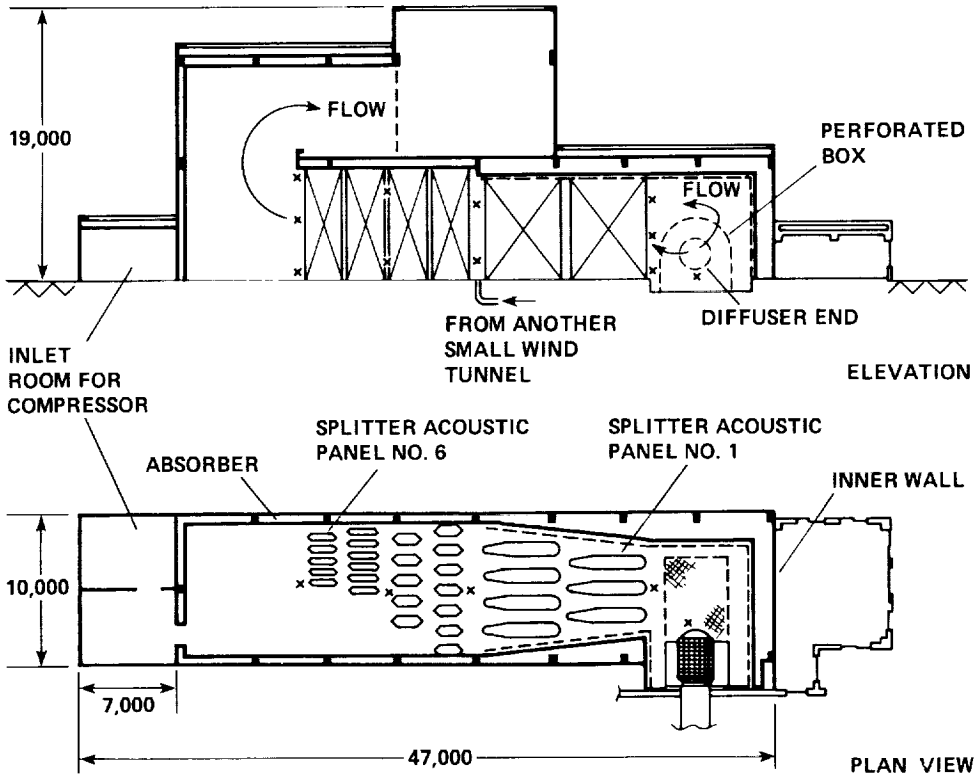

Figure 18.– Multi-row acoustic baffles in the NAL Transonic Wind Tunnel (Tokyo) (refs. 33 and 34).

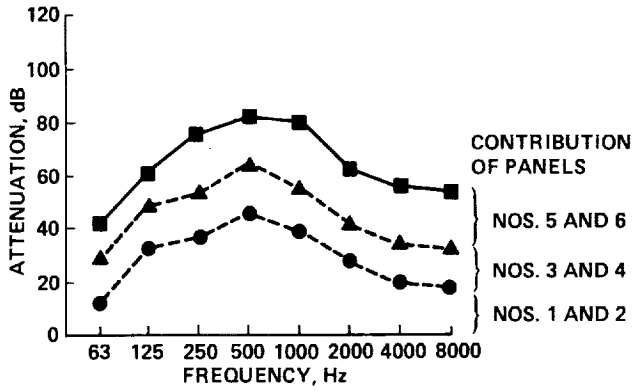

a) Attenuation of baffles in NAL Transonic Wind Tunnel (fig. 18) (refs. 33 and 34).

Figure 19.– Continued.

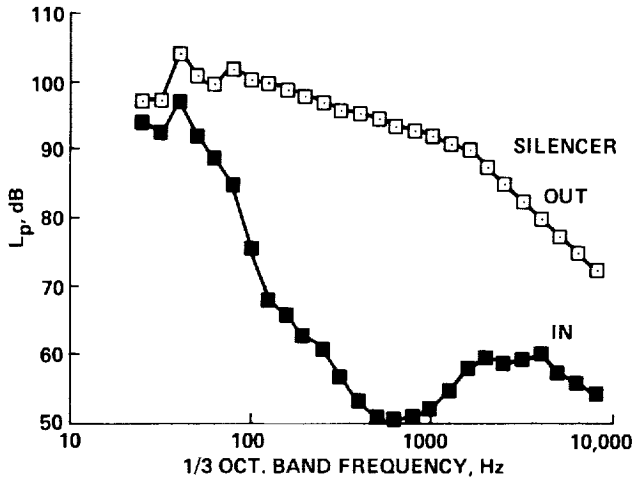

b) Panels 1 and 2 attentuation applied to 80×120 background noise (fig. 17).

Figure 19.– Concluded.

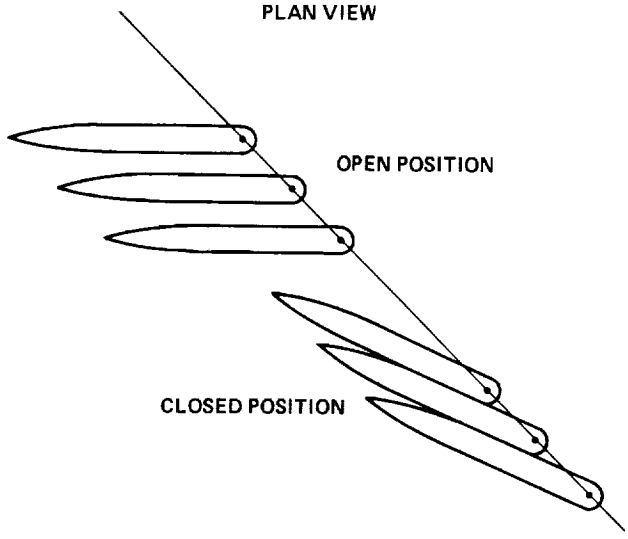

Figure 20.– Open and closed positions for acoustic baffles at vane set 4 (50% blockage).

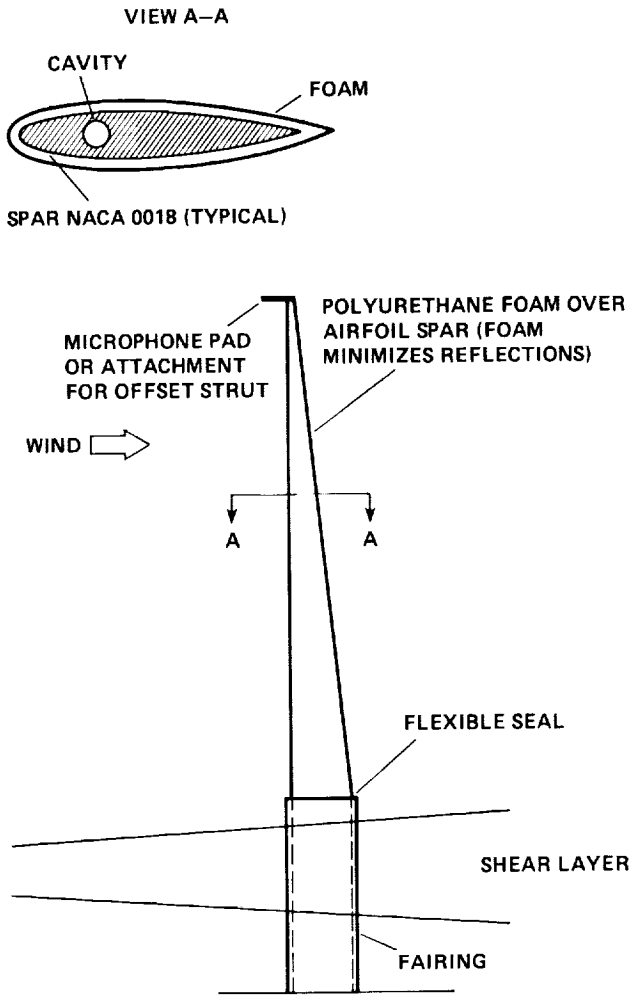

Figure 21.– Tapered strut designed to span a shear layer with minimal noise and vibration. Microphone leads pass inside the strut.

NASA
National Aeronautics and Space Administration

Report Documentation Page

1. Report No.	2. Government Accession No.	3. Recipient's Catalog No.
NASA TP-3020		

4. Title and Subtitle

Large-Scale Aeroacoustic Research Feasibility and Conceptual Design of Test-Section Inserts for the Ames 80- by 120-Foot Wind Tunnel

5. Report Date

December 1990

6. Performing Organization Code

7. Author(s)

Paul T. Soderman and Larry E. Olson

8. Performing Organization Report No.

A-88007

10. Work Unit No.

307-50-62-11

9. Performing Organization Name and Address

Ames Research Center
Moffett Field, CA 94035-1000

11. Contract or Grant No.

13. Type of Report and Period Covered

Technical Paper

12. Sponsoring Agency Name and Address

National Aeronautics and Space Administration
Washington, DC 20546-0001

14. Sponsoring Agency Code

15. Supplementary Notes

Point of Contact: Paul Soderman, Ames Research Center, MS 247-2, Moffett Field, CA 94035-1000
(415) 604-6681 or FTS 464-6681

16. Abstract

An engineering feasibility study was made of aeroacoustic inserts designed for large-scale acoustic research on aircraft models in the 80- by 120- Foot Wind Tunnel at NASA Ames Research Center. The advantages and disadvantages of likely designs were analyzed. Results indicate that the required maximum airspeed leads to the design of a particular insert. Using goals of 200, 150, and 100 knots airspeed, the analysis indicated a 30- × 60-ft open-jet test section, a 40- × 80-ft open-jet test section, and a 70- × 10-ft closed test section with enhanced wall lining, respectively. The open-jet inserts would be composed of a nozzle, collector, diffuser, and acoustic wedges incorporated in the existing 80×120 test section. The closed test section would be composed of approximately 5-ft acoustic wedges covered by a porous plate attached to the test-section walls of the existing 80×120. All designs would require a double row of acoustic vanes between the test section and fan drive to attenuate fan noise and, in the case of the open-jet designs, to control flow separation at the diffuser downstream end. The inserts would allow virtually anechoic acoustic studies of large helicopter models, jets, and V/STOL aircraft models in simulated flight. Model scale studies would be necessary to optimize the aerodynamic and acoustic performance of any of the designs. In all designs studied, the existing structure would have to be reinforced. Successful development of acoustically transparent walls, though not strictly necessary to the project, would lead to a porous-wall test section that could be substituted for any of the open-jet designs, and thereby eliminate many aerodynamic and acoustic problems characteristic of open-jet shear layers. The large size of the facility would make installation and removal of the insert components difficult. Consequently, scheduling of the existing 80×120 aerodynamic test section and scheduling of the open-jet test section would likely be made on an annual or longer basis. The enhanced wall-lining insert would likely be permanent. Although the modifications are technically feasible, the economic practicality of the project has not been evaluated.

17. Key Words (Suggested by Author(s))	18. Distribution Statement
Aeroacoustics, Acoustics, Wind tunnel Wind tunnel design Wind tunnel performance	Unclassified-Unlimited Subject Category – 71

19. Security Classif. (of this report)	20. Security Classif. (of this page)	21. No. of Pages	22. Price
Unclassified	Unclassified	52	A03

NASA-Langley, 1990